Investigating Brain Function using Functional MRI-based Meta-analysis and Diffusion Tensor Imaging

by

Madhura Baxi

A thesis submitted to the Graduate Faculty of
Auburn University
in partial fulfillment of the
requirements for the Degree of
Master of Science

Auburn, Alabama
May 10, 2015

Keywords: Diffusion Tensor Imaging, Depression, Suicide, Canine, Meta-analysis, Default Mode Network

Approved by

Gopikrishna Deshpande, Chair, Associate Professor, Electrical & Computer Engineering
Thomas S Denney, Director, Auburn University MRI Research Center
Jennifer L Robinson, Assistant Professor, Department of Psychology

Abstract

The investigation of structure and function in biological systems, specifically the brain, is paramount given the close relationship that they share with each other. Functional magnetic resonance imaging (fMRI) and Diffusion Tensor Imaging (DTI) are two non-invasive MR-based modalities which are popular for investigating function and structure, respectively. In this thesis, we present novel advances in fMRI and DTI post-processing which will likely hasten the widespread use of these modalities for understanding brain function. Specifically, in the first application, Activation Likelihood Estimation meta-analyses (a popular statistical method used for assimilating results across many fMRI studies) along with meta-analytic connectivity modeling and DTI were assembled in a novel analysis pipeline in order to identify the neural substrates underlying gender differences in all forms of suicidal behavior in an attempt to form specific new hypotheses which can be tested in future experimental studies. In the second application, DTI was used in a dog model for generating a voxel-specific atlas of tensor (and hence, axonal) orientations by adapting existing human pipelines to dog data. Further, probabilistic tractography was utilized to test the hypothesis that previously seen anterior-posterior dissociation in the Default Mode Network (DMN) in dogs in a resting state fMRI study could have a structural basis. Contrasting anterior-posterior DMN connectivity in dogs with that in humans may help us understand the evolutionary role of the DMN.

Acknowledgments

First, I would like to express my eternal gratitude to my parents for their everlasting support and love. They made me into who I am and I would like to dedicate my thesis to them.

I would like to thank my advisor Dr. Gopikrishna Deshpande, for introducing me to the cutting edge research field of neuroimaging. I have learnt the vital skill of critical thinking from him. I am grateful to him for his patience, support and invaluable advice all through the thesis research.

I would like to thank Dr. Jennifer Robinson for the time she dedicated to help me learn Diffusion Tensor Imaging (DTI) technique. The hands-on practical sessions in a course taken by her proved extremely beneficial in my research work for Master's thesis.

I would like to extend my sincere thanks to Dr. Thomas Denney for agreeing to serve on my graduate committee and review my thesis work. I take this opportunity to thank my friends at the AU MRI center, especially, Karthik, Pruthvi, Hao and Xiaoxia who helped me a lot at the beginning of my graduate studies.

I am immensely grateful to Dr. Yogesh Rathi and Dr. Marek Kubicki who offered me an opportunity to work at Psychiatry Neuroimaging Lab, HMS, one of the premier research labs in the field of neuroimaging, especially DTI during my Master's program.

I would like to thank Rasika, Amanda, Suhrid, Shruti and most importantly my late close friend Astha Pareek for their ceaseless encouragement and support.

Table of Contents

List of Tables

List of Figures

Chapter 1: Introduction

1.1 MRI

Magnetic Resonance Imaging (MRI) is a non-invasive imaging technique to investigate anatomy and physiology of the body. It is nowadays extensively used to diagnose and treat medical conditions. MRI uses a powerful magnetic field. A large number of hydrogen nuclei (single protons) are present in our brain, continuously spinning around an arbitrary axis. These spinning protons possess magnetic moment according to the laws of physics. Under normal circumstances these moments have no fixed orientation so there is no net magnetic field (Fig. 1.1B). But on application of an external static magnetic field B0 (Fig. 1.1A) such as during Magnetic Resonance Imaging, the majority of the protons begin to align themselves in the direction of the magnetic field and a few align themselves opposite to it and start to precess about this external field (Fig. 1.1C). This leads to a net magnetization in the direction of the external magnetic field B0. Radio frequency (RF) coils are used to transmit B1 magnetic field perpendicular to B0. The frequency of RF pulse is the resonant frequency of the hydrogen nuclei. If the pulse is applied for sufficient time, the spins are flipped from the longitudinal plane into the transverse plane towards the direction of the coil. The RF pulse is then turned off and the signal can be detected by the RF receiver coil. These spins then flip back into the longitudinal plane increasing the magnetization in the direction of B0 field. This recovery is called T1 recovery. The decay of magnetization in the direction of B1 field is called T2 decay. The signal is at its peak at the point when RF pulse is switched off, but decays very quickly due to longitudinal relaxation or T1 recovery and transverse relaxation or T2 decay. The faster decay due to magnetic field inhomogeneities is called a free induction decay (FID) with a time constant $T2^*$. In T2 decay, spins begin to dephase due to individual spins perceiving the local differences

in the magnetic field caused by interactions between them. Spins then begin to precess at slightly different rates (Fig. 1.1D). In order to recover this decayed signal, a refocussing RF pulse is applied to flip the spins 180^0. Phase position of each spin is inverted such that the spins that were precessing faster are now behind the spins that were precessing slower. The precession rates still being the same, finally catch each other up after some finite time, resulting in a spin-echo. This spin-echo is attained at the echo-time, TE. The contrast of the MRI images is determined by the combination of T1, T2 relaxation times and pulse sequences such as spin echo and gradient echo sequences [1] [2] [3].

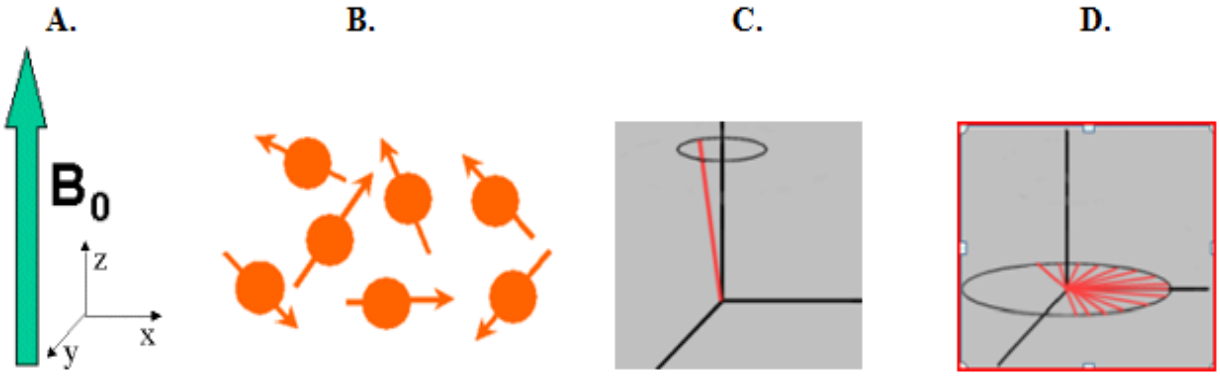

Figure 1.1 *A. Static external magnetic field applied during MRI. B. Protons randomly aligned in the absence of external magnetic field thus not producing any magnetic field analogous to a spinning top. C. In the presence of external magnetic field protons begin to precess about the B0 field. D. After removing the RF pulse, spins begin to dephase and begin to precess at slightly different rates consequently resulting in an increased dispersed distribution around the clock face.* **[4]**

Gradient coils are used to obtain spatial information. The coils cause the gradient in the magnetic field causing the nuclei at different locations to rotate with different speeds, in turn providing the spatial information. MRI technique provides us with 3D high spatial resolution images without the use of harmful radiations. Hence, MRI is one of the promising diagnostic imaging techniques of this decade.

1.2 Functional MRI

Functional Magnetic Resonance Imaging is an MRI technique used to map neuronal activity to investigate brain function over time [5]. fMRI is an indirect measure of neural activity as it is mainly based on the blood oxygenation level dependent (BOLD) contrast. fMRI utilizes the differences between magnetic susceptibities of oxygenated and de-oxygenated hemoglobin for the image contrast. Blood containing deoxyhemoglobin is more paramagnetic than the surrounding tissue whereas blood containing oxyhemoglobin is slightly more diamagnetic than water. Neuronal activation in a brain region causes increase in metabolic demand of that region. This leads to increase in blood flow to that region in order to fulfil the increased requirement of oxygen. Increased blood flow in the area triggers sudden increase in the oxygenated hemoglobin and relative decrease in deoxygenated hemoglobin concentration. This change in the concentration of oxygen in the blood induces small magnetic field variations in the blood as well as in the surrounding extra-vascular area. Hydrogen nuclei (protons) in these regions sense these field distortions, which are reflected in the signal decay process, characterized by T2 (spin echo) or T2* (gradient echo) decay [6]. MRI thus detects the differences in the oxygenation level of blood upon neural firing and depicts it in the form of image intensity in the MRI scans. The change in MR signal from neuronal activation is called hemodynamic response (HDR). HDR lags 1 to 2 seconds behind the neural activation that triggered it and peaks after around 5 seconds. BOLD response is modelled by convolving the hemodynamic response with the series of impulses representing neuronal activity. BOLD was suggested for potential use in functional study of the brain [7]. fMRI offers a spatial resolution in the order of millimeters but has a poor temporal resolution usually between 1 to 2 seconds compared with some other neuroimaging techniques such as electroencephalography (EEG) and magnetoencephalography (MEG). Its high

spatial resolution is an interesting and beneficial characteristic and thus has been extensively used in both research and clinical applications.

1.3 Diffusion Tensor Imaging

Diffusion Tensor Imaging (DTI) is a recently developed Magnetic Resonance Imaging (MRI) method that can provide us with a description of microstructural changes or differences with neuropathology. DTI is a non-invasive method that measures the anisotropic diffusion of water molecules in biological tissue. This method is now widely used in research to investigate brain structure by mapping the water diffusion in brain at microscopic level. As DTI measures directional distribution of water diffusivity, it is being extensively used to investigate microarchitecture of the white matter (WM) fiber tracts in the brain which is not assessable with conventional MR imaging.

1.3.1 Diffusion Weighted Magnetic Resonance Imaging

Random translational motion of molecules that results from the thermal energy carried by these molecules is called Brownian motion [8]. In a homogeneous barrier-free medium, diffusion follows Brownian motion. Water molecules in brain tissue follow three types of diffusion – Free diffusion, Restricted Isotropic diffusion and Restricted anisotropic diffusion [9]. Free diffusion of water molecules primarily occurs in Cerebrospinal Fluid in the brain (Fig. 1.2A). Whereas within tumor at high cell density, reduced extracellular space and cell membrane act as a barrier to water movement. This results in restricted isotropic diffusion (Fig. 1.2B). The third type of diffusion i.e. restricted anisotropic diffusion (Fig. 1.2C) takes place due to obstacles created by certain structured tissues such as nerve fibers (bundles of axons running in parallel, with concentric layers of myelin restricting transversal diffusion) that orient the motion of water

molecules in certain specific spatial directions. Diffusion Weighted MRI (DWI) uses these differences in water molecule mobility to reveal microscopic details of tissue architecture.

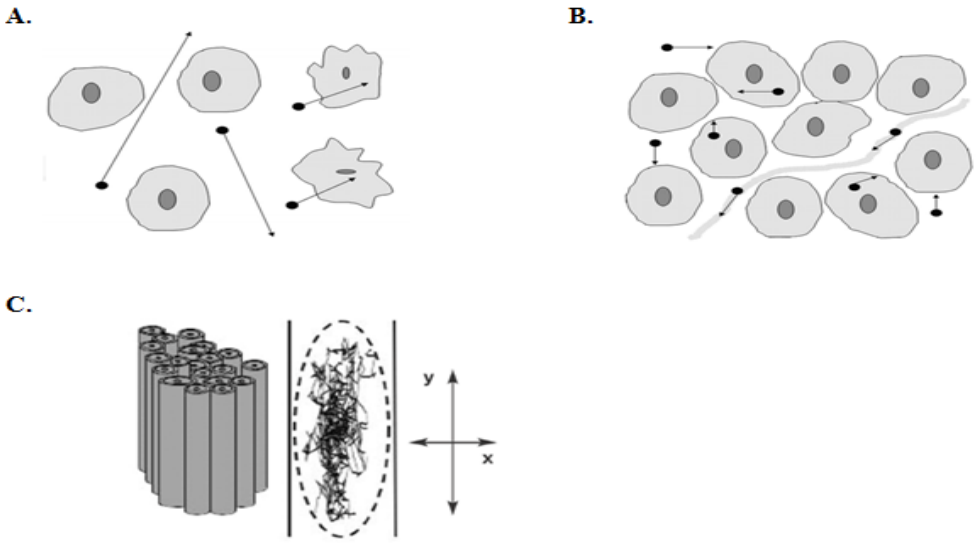

Figure 1.2 *Black dots in (A) and (C) represent water molecules. Water molecules are present in extracellular space, intracellular space and intravascular space in the brain. The environment water molecules are present in, defines the type of diffusion the molecules undergo.* ***A.*** *Free diffusion of water molecules occurs in less cellular environment such as Cerebrospinal fluid.* **[10]** ***B.*** *Highly cellular environment restricts the motion of water molecules resulting in restricted isotropic diffusion.* **[10]** ***C.*** *Certain structured tissues such as nerve fibers allow water diffusion to occur only in certain spatial directions thus giving rise to restricted anisotropic diffusion.* **[11]**

Diffusion Weighted MRI provides image contrast that depends upon the random microscopic motion of water protons, which may be significantly altered by different pathological process. DW-MRI uses a T2-weighted pulse sequence with two extra gradient pulses of equal amplitude but opposite polarity. Stationary tissue gets rephased and dephased equally. However, the spins that moved during this interval of time suffer a net dephasing and signal loss [9]. So higher the water diffusion rate, the attenuation of signal is greater, in turn causing that region of the brain to appear darker in the DW image. Imaging is more sensitive to molecular motion in the direction of the additional applied gradients.

1.3.2 Diffusion Tensor

Anisotropic diffusion of water occurs three to six times faster along the direction of the axonal tract than in the perpendicular direction [12]. Thus, in order to ascertain good contrast and to be able to discern anisotropy due to diffusion along certain structures or fibers, 6 combinations of gradient pairs [13] are essential to obtain a 3 dimensional depiction of diffusion by computing Tensor [14] [15]. Estimated tensor provides Apparent Diffusion Coefficients (ADCs) along the scanner's coordinate system. Therefore, the estimated tensor for each voxel is diagonalized to acquire ADCs along a local coordinate system in each voxel, determined by the anatomy.

$$D = [v1|v2|v3]^{T} \begin{bmatrix} \lambda 1 & 0 & 0 \\ 0 & \lambda 2 & 0 \\ 0 & 0 & \lambda 3 \end{bmatrix} [v1|v2|v3]$$

Where D represents the estimated tensor, v1, v2 and v3 represent the eigenvectors that form the orthonormal basis for diffusion in each voxel and $\lambda 1$, $\lambda 2$, $\lambda 3$ denote the eigenvalues (ADCs) along these 3 directions [16]. V1 represents the principle eigenvector, direction of maximum diffusivity and $\lambda 1$ represents the diffusivity in that direction. Tensor derived metrics can be computed using the estimated diffusion tensor. The metrics include fractional anisotropy (FA) maps, mean diffusivity (MD) maps, axial diffusivity (AD) and radial diffusivity (RD) [17]. Computing the mean of all eigenvalues provides us with mean diffusivity map (MD). Fractional anisotropy (FA) map is obtained by calculating the variance of three tensor eigenvalues, normalized to take values between 0 and 1 [18]. FA encodes the degree of anisotropy and tells us how strongly directional diffusion is. FA map contains higher values in white matter due to high anistropic diffusion in this region. Color FA map provides an improved visualization by using the principle eigenvector of the diffusion tensor and can be further used for diffusion-tensor tractography. Diffusion direction in this color map is coded by color.

1.3.3 Tractography

DTI fiber tracking (DTI-FT) is utilized for quantitative assessment of specific neuronal pathways [19] [20]. It determines inter-voxel connectivity on the basis of the anisotropic water diffusivity. In each brain voxel, the dominant direction of axonal tracts is assumed to be in the orientation of primary eigenvector of the diffusion tensor. Fiber tracking (FT) uses the diffusion tensor of each voxel to follow an axonal tract in 3D from voxel to voxel. FT can be done using deterministic method such as FACT algorithm or probabilistic method. However probabilistic FT is preferred over deterministic tractography due to 3 major reasons: - (i) Deterministic FT entails harsh stopping criteria (ii) Diffusion tensor is utilized to indicate local diffusion direction (iii) Deterministic FT does not allow uncertainty of diffusion direction, consequently is unable to resolve crossing fibers [21]. Probabilistic method on the other hand incorporates the expected uncertainty into the tracking algorithm by computing probability density function (pdfs) of the orientation of a neuronal fiber estimated with an empiric function based on the FA and Bayesian model [22]. Multiple pathways arising from seed voxel are depicted and then probability of dominant streamline passing through any single region is computed. Samples are generated from local pdfs at each voxel. Thus, connectivity probabilities are estimated between seed and target voxels by repetitive sampling streamlines through the local pdf. Diffusion tensor imaging-FT is beneficial for surgical planning as well as for postoperative assessment [21]. With co-registration of DTI-FT to the high resolution anatomic images, we can use these techniques for surgical navigation. Tractography is a promising technique used to investigate neurological conditions that affect white matter integrity such as Multiple Sclerosis [23] and frequently used for modelling the structural connectivity in the brain.

1.4 Meta-analysis

Activation likelihood estimation (ALE) algorithm [24] [25] [26] is a widely used probabilistic approach for co-ordinate based meta-analysis. Importantly, ALE accounts for the spatial uncertainties associated with different subjects and brain templates. In the ALE approach, every focus that is reported to be activated in an experiment yields an estimated 3D probability distribution with the center of distribution being at the focus. The ALE scores for each voxel are calculated by the union of activation probabilities for each voxel. The activation probability of a given focus at a voxel is calculated using a Gaussian probability function P.

$$P = \frac{e^{\frac{-d^2}{2\sigma^2}}}{(2\pi)^{0.5}\,\sigma}$$

Where d is the Euclidean distance from center of voxel to particular focus, σ is the standard deviation of the probability distribution. The σ values are calculated using the Euclidean distance between the same focus in different subjects. After obtaining the ALE scores of all voxels present in the brain, they are then compared with a null-distribution. The null-distribution is obtained by calculating ALE scores of voxels when there is no biological activity in the brain. By comparing the activation-related ALE score of voxels with the null distribution, a thresholded activation map can be generated [24] [25] [26].

1.5 Organization of Thesis

fMRI is a neuroimaging technique using MRI technology for non-invasive mapping of brain activity at a spatial resolution in the order of millimeters within a matter of seconds. Therefore, fMRI is a powerful tool that is used for detecting functional activation within the brain and for

understanding human cognitive processes. Meta-analysis is a statistical method which is used to assimilate results from a multitude of such neuroimaging studies in the anticipation of identifying interesting patterns or relationships in the light of multiple studies. It is a popular tool for summarizing results across many fMRI studies. Diffusion Tensor Imaging (DTI) is another recently developed noninvasive Magnetic Resonance Imaging (MRI) method that is now widely used in research to investigate brain structure by mapping the water diffusion in brain at microscopic level, consequently allowing us to reconstruct axonal tracts in 3D.

The aim of this thesis is to employ the powerful techniques of functional MRI-based meta-analysis and diffusion tensor imaging to study the brain function in humans as well as canines in two separate studies. Chapter 2 presents the study conducted for investigating the relationship between the gender differences and all forms of suicidal behavior, fatal as well as non-fatal. Co-ordinate based meta-analysis method namely; Activation Likelihood Estimation (ALE) was used in this chapter to explore and identify the neural substrates underlying fatal suicidal behavior and to distinguish between the neural activations for fatal and non-fatal suicide. Additionally, diffusion tractography was utilized in this thesis to investigate gender differences in the structural networks pertaining to fatal and non-fatal suicide in humans. Thus, both functional and structural networks corresponding to fatal suicidal behavior were analyzed in an attempt to form a basis for future experimental studies investigating gender differences relating to both forms of suicide. In chapter 3, diffusion tensor imaging and tractography was used to create a DTI-based atlas and explore the structural connectivity in the canine model between two major hubs of the Default Mode Network, namely Anterior Cingulate Gyrus (ACC) and Posterior Cingulate Gyrus (PCC). Chapter 4 summarizes the work in this thesis in the form of a conclusion.

Chapter 2: A Neural Basis for the Acquired Capability for Suicide

My contribution to this study was performing the meta-analysis, generating and compiling the results and writing the bulk of the description of methods, results and discussion. I extend my acknowledgment to Dr. Witte for contributing her expertise in IPTS and ACS to guide the analysis as well as writing descriptions relevant to them. I acknowledge Dr. Robinson for initially performing DTI analysis and later guiding me for completing DTI analysis as well as for writing descriptions of DTI acquisition/analysis and meta-analysis. I also acknowledge Dr. Glahn's contribution of DTI data used in this work and Dr. Deshpande for overall guidance regarding the idea as well as guiding me for writing the descriptions.

Abstract

The high rate of fatal suicidal behavior in men is an urgent issue as highlighted in the public eye via news sources and media outlets. In this study, we have attempted to address this issue and understand the neural substrates underlying the gender differences in the rate of fatal suicidal behavior. The Interpersonal-Psychological Theory of Suicide (IPTS) has proposed an explanation for the seemingly paradoxical relationship between gender and suicidal behavior, i.e. greater non-fatal suicide attempts by women but higher number of deaths by suicide in men. This theory states that possessing suicidal desire (due to conditions such as depression) alone is not sufficient for a lethal suicide attempt. It is imperative for an individual to have acquired the capability for suicide (ACS) along with suicidal desire in order to die by suicide. Therefore, higher levels of ACS in men may explain why men are more likely to die by suicide than women, despite being less likely to experience suicidal ideation or depression. In this study, we used activation likelihood estimation meta-analysis to investigate a potential ACS network that involves neural substrates underlying emotional stoicism, sensation seeking, pain tolerance, and

fearlessness of death along with a potential depression network that involves neural substrates that underlie clinical depression. Brain regions commonly found in ACS and depression networks for males and females were further used as seeds to obtain regions functionally and structurally connected to them. We found that the male-specific networks were widespread and diverse than the female-specific ones. Also, while the former involved motor regions such as the premotor cortex and cerebellum, the latter was dominated by limbic regions. This may support the fact that suicidal desire generally leads to fatal/decisive action in males while in females, it manifests as depression, ideation and generally non-fatal actions. The proposed model is a first attempt to characterize the neural networks underlying gender differences in suicidal behavior. Future studies should examine the proposed network to better characterize and refine this network using tasks specifically targeted toward constructs underlying ACS.

2.1 Introduction

Each year in the United States, over 40,000 individuals die by suicide [27]. These figures do not include non-fatal suicide attempts, which are estimated to occur 25 times more frequently than fatal suicide attempts [27]. One of the most well established, and yet paradoxical findings with regard to the epidemiology of suicidal behavior is that men are far more likely to die by suicide than women are [28], despite the fact that they are significantly less likely to experience depression (e.g., [29] [30]), suicidal ideation [31], and nonfatal suicide attempts [31]. Although men tend to choose more lethal methods than women do [32] [33], a recent study has demonstrated that even among those who choose the same method, men are more likely than women are to have a fatal outcome [34]. Thus, method selection alone cannot explain the observed gender differences in fatal suicidal behavior.

2.1.1 Neural Mechanisms of Suicide.

The neural basis of suicidal behavior has been explored using structural [35] [36] [37], functional [38] [39], and metabolic imaging [40] [41]. However, research on this topic often does not provide a satisfactory explanation for the observed sex differences in both non-fatal and fatal suicidal behavior.

One conclusion from the existing literature is that prefrontal hypo-activity [42], which is modulated by decreased serotonin binding in the prefrontal cortex [43], is implicated in suicidal behavior. However, hypo-activity in the prefrontal cortex is associated with a range of psychopathology, including depression [44], posttraumatic stress disorder [45], and schizophrenia [46]. Thus, the specificity of this risk factor for suicidal behavior is unclear. Additionally, there is evidence that women have decreased serotonin binding in the prefrontal cortex compared to men (e.g., [47] [48]). This pattern suggests that prefrontal hypoactivity may explain the elevated risk for non-lethal suicidal behavior in women. However, this risk factor does not provide a satisfactory explanation for the elevated risk for lethal suicidal behavior in men. It is not surprising that the identified neural substrates for suicidal behavior are plausible explanations for female vulnerability, as virtually all of the existing research has focused on non-fatal suicidal behavior. In a recent review of functional and structural brain studies of suicidal behavior [43], 21 of the 22 articles included were comparisons between non-fatal suicide attempters and controls. Given the association between female gender and non-fatal suicide attempts, conclusions from these research studies are not particularly informative regarding neural substrates that may explain the association between male gender and fatal suicide attempts.

Research on the neural substrates of fatal suicidal behavior is hampered by the difficulty of conducting research on individuals who die by suicide. Indeed, brain imaging research on suicide decedents is impossible, unless pre-morbid imaging data are available, as was the case in the sole imaging study that has examined suicide decedents [49]. To date, this difficulty has been addressed by using non-fatal suicide attempts as a proxy for fatal suicidal behavior. This is problematic, as this approach will not uncover neural activations that distinguish fatal versus non-fatal suicidal behavior, which may explain the gender paradox in suicidal behavior that was presented above.

As an alternative to using non-fatal suicide attempts as a proxy for fatal suicide attempts, some have proposed the investigation of endophenotypes for suicidal behavior (i.e., discrete, measurable traits that mediate the link between genetic risk and a particular form of pathology; [50]. Given the heterogeneity of various forms of suicidal behavior, the complex interplay between biological and environmental risk factors and the difficulty in conducting research on fatal suicidal behavior, focusing on endophenotypes may prove promising in elucidating biological risk factors for suicide. Several endophenotypes for suicide have been identified to date (e.g., impulsive aggression, disadvantageous decision making; [50]). However, [50] state the need for research that investigates gender differences in the neurobiology of suicidal behavior, an aspect that has not been thoroughly investigated.

2.1.2 The Interpersonal-Psychological Theory of Suicide.

Although [50] propose some promising endophenotypes for suicide, the existing literature on this topic is atheoretical. The benefits of grounding empirical research in theory are numerous; in this particular case, we propose that using a comprehensive account of suicide as a theoretical framework would integrate what is already known while fostering novel predictions. One theory

that appears promising in this regard is the interpersonal-psychological theory of suicide (IPTS), which was formulated to explain the manifestation of suicidal behavior and prompt empirical investigation [51] [52]. Perhaps more so than any other suicide-related theory to date, the IPTS proposes a plausible explanation for the seemingly paradoxical relationship between gender and all forms of suicidal behavior. According to the IPTS, even individuals who experience intense suicidal desire will not die by suicide without the fearlessness about death and pain tolerance necessary to endure the act of making a lethal suicide attempt. Together, fearlessness about death and physical pain tolerance comprise a novel construct first introduced by [51], known as the acquired capability for suicide (ACS). Once developed, the ACS is proposed to remain fairly stable over time [51]. Therefore, an individual who has developed this capability is at high risk for making a lethal suicide attempt, should he or she develop a desire for suicide at a later point in time.

According to the IPTS, suicidal desire stems from the simultaneous presence of thwarted belongingness (i.e., loneliness and lack of reciprocal care) and perceived burdensomeness (i.e., feeling like a liability on others and self-hatred). It is only when a desire for suicide simultaneously occurs with the acquired capability for suicide that a lethal suicide attempt is even possible. As articulated by [53], one can acquire the capability for suicide regardless of the presence of suicidal desire. Thus, the ACS is distinguishable from suicidal ideation. Expanding upon this point, it is possible that vulnerabilities for acquiring the capability for suicide are distinct from vulnerabilities for developing suicidal desire.

The IPTS offers the following explanation for gender differences in non-fatal and fatal suicidal behavior: women are more likely to experience perceived burdensomeness and/or thwarted belongingness, and men are more likely to acquire the capability for suicide. Regarding

the first point, [54] propose that women are more likely than men to experience interpersonal difficulties (e.g., [55]), and they may be more likely than men to experience decrements in self-esteem (c.f., self-hatred) stemming from interpersonal difficulties. This may make women more vulnerable to experiencing both perceived burdensomeness and thwarted belongingness, and therefore, suicidal desire. In contrast, although men may be less likely than women to experience suicidal desire, they are proposed to be more likely to acquire the capability for suicide [51] [52] – a proposition that has borne out in behavioral literature [56] [57]. Consequently, men who experience suicidal desire are more likely to have a fatal outcome than women with similar levels of suicidal desire.

There are two main explanations for why men may have higher acquired capability for suicide than women do. According to the IPTS, the capability for lethal self-harm is acquired primarily through exposure to life experiences that are painful and provocative, which result in habituation to fear of death and/or physical pain. Examples of experiences that are proposed to serve this function include impulsive/aggressive behaviors and combat exposure, both of which are positively associated with measures of acquired capability for suicide [58] [59] and death by suicide (e.g., [60] [61]). These experiences are also more common among men, which is consistent with [51] proposition that men may be more likely to encounter experiences that habituate them to fear of death and physical pain over the course of their lifetime.

Although exposure to painful and provocative experiences is proposed as the primary mechanism by which one acquires the capability for suicide, it is not the only one. The IPTS allows for the possibility that various neurobiological and temperamental factors may make an individual more likely to fully acquire the capability for suicide over the course of his/her lifetime [52]. A recent study [57] examined sensation seeking and emotional stoicism as

potential temperamental characteristics that explain the relationship between gender and both facets of ACS. Across two large, independent samples, sensation seeking accounted for the relationship between gender and fearlessness about death, and stoicism fully accounted for the relationship between gender and physical pain insensitivity. Thus, these temperamental characteristics may explain the observed gender differences in the ACS, and therefore, greater likelihood of death by suicide among men.

Findings in [57], when viewed within the purview of IPTS, suggest a possible brain network that may explain the biological basis for the gender differences in lethal suicidal behavior (SB). We hypothesize that this network would involve neural substrates that underlie emotional stoicism, sensation seeking, pain tolerance, and fearlessness about death, all of which may be considered endophenotypes for fatal suicide attempts. Our proposed brain network is based on a body of literature suggesting that these constructs are interconnected. Numerous studies have demonstrated an association between male gender and both stoicism and sensation seeking [62] [63] [64] [65]. Additionally, several studies have established the link between stoicism and pain tolerance (e.g., [66] [67] [68] [57] [69]). Likewise, sensation seeking has been found to be an important correlate of acquired capability for suicide, as two studies have demonstrated associations between sensation seeking and the acquired capability for suicide (ACS; [58] [57]). Given the overlapping theoretical constructs, the current study represents the first investigation of the neural substrates that may underlie gender differences in lethal SB.

As noted above, the existing research on the neural basis of suicidal behavior is limited, and is largely focused on factors that explain the increased risk for non-fatal suicidal behavior seen in women, without providing an adequate explanation for the increased risk for death by suicide seen in men. By parsing out suicidal desire and capability for suicide, the IPTS offers a useful,

theoretically driven framework suggesting the possibility of separate neural substrates underlying the theoretical constructs. In this study, we hope to address the two aforementioned challenges in this area of research by distinguishing the neural substrates for ACS from neural substrates relevant to suicidal desire, and attempting to explain the higher suicide mortality seen in men in terms of gender differences of underlying neural substrates. In order to do so, we conducted two separate activation likelihood estimation meta-analyses. The first focused on our proposed acquired capability for suicide brain network by finding brain regions commonly activated by at least two of the four tenets of ACS: emotional stoicism, sensation seeking, pain tolerance and fearlessness of death. Our second meta-analysis focused on brain regions activated by clinical depression since it is intricately linked to suicidal desire. The intersection of these two followed by meta-analytic connectivity modeling provided us with an ACS-Depression network which may underlie lethal suicide attempt and which is distinct in males and females. Further, we performed structural connectivity analysis using diffusion tensor imaging (DTI) for demonstrating that this ACS-Depression network has different structural connectivity patterns in males and females. We show that the meta-analyses coupled with insights from DTI leads to testable hypotheses regarding the neural basis of IPTS.

2.2 Methods

2.2.1 Activation Likelihood Estimation

Activation likelihood estimation (ALE) algorithm [24] [25] [26] was used to investigate brain regions mediating gender differences underlying ACS and depression. We searched the BrainMap database for papers coded with specific search criteria, described below, using the Sleuth search portal [70] [71] [72]. The BrainMap database archives whole-brain coordinates

from functional neuroimaging studies using a rigorous coding scheme [72] [73]. Coordinates of activation from contrasts meeting our criteria were then downloaded, and meta-analytic statistics were computed using GingerALE software [24] [25] [26] to determine regions of convergence amongst our search set using the ALE algorithm described in the previous chapter. Resultant ALE maps were thresholded with a minimum cluster size of 100 mm^3 and a p-value of 0.05, corrected for false positives using false discovery rate [74]. All searches had the basic criteria of including only activations for both ACS and Depression and only normal subjects in the case of ACS whereas only depressed in the case of Depression. All searches were performed for males and females separately. In order to form a functional neural network for ACS, different ALE meta-analyses were performed using search criteria related to (i) emotion (i.e., all aforementioned search criteria plus 'Experiments – Behavioral domain – Emotion – All subtypes' giving us for males: 446 experiments, 2145 subjects and for females: 355 experiments, 149 subjects to be used for ALE meta-analyses) (ii) pain processing (i.e., all basic search criteria plus 'Experiments – Behavioral domain – Perception – Somesthesis Pain', giving us for males: 79 experiments, 372 subjects and for females: 34 experiments and 178 subjects to be used for ALE meta-analyses); (iii) sensation seeking (i.e., all basic search criteria and experiments with paradigm class as reward, given the intimate association between sensation seeking and the brain's reward system, giving us for males: 127 experiments and 621 subjects and for females: 35 experiments and 174 subjects to be used for ALE meta-analyses); (iv) fear (i.e., all basic search criteria in addition to 'Experiments – Behavioral domain – Emotion – Fear', giving us for males: 54 experiments and 318 subjects and for females: 32 experiments and 231 subjects to be used for ALE meta-analyses). Each of these searches was run separately. The above search criteria are motivated by the four main constructs underlying IPTS as outlined in

the introduction, i.e. emotional stoicism, sensation seeking, pain tolerance, and fearlessness of death. It is noteworthy that using these exact terms in the Sleuth search would give very few or no relevant papers. Therefore, we searched for broader concetualizations of these constructs. For example, we believe that the extent of activation in the fear-related regions might be an important factor modulating fearlessness of death, and hence, we used 'Experiments – Behavioral domain – Emotion – Fear' as the search criterion. The ACS was proposed with two constructs, fearlessness of death and pain tolerance. However, a recent study [57] examined sensation seeking and emotional stoicism as potential temperamental characteristics that explain the relationship between gender and both facets of ACS. Therefore, as the prevalence of at least 2 of the 4 constructs underlying IPTS might account for acquired capability for suicide, we deemed all voxels that were activated by 2 or more of the search conditions to represent the functional neural network in males and females separately for ACS (we will call this "ACS network").

In order to obtain the functional neural network for depression, ALE meta-analyses were performed using search criteria related to depression. Two Sleuth searches were performed, one for males and the second for females. Common search criteria used for both of the searches were subjects diagnosed with depression (Subjects – Diagnosis – Depression) and experiments showing only activations as results (Experiments – Activations only), giving us for males: 31 experiments and 112 subjects and for females: 29 experiments and 149 subjects to be used for ALE meta-analyses. Additional criterion used for the first search was only male subjects (Subjects – Gender – Males only) and the second search was for only female subjects (Subjects – Gender – Females only). The resultant ALE map from this search was interpreted as a representation of the functional neural network in males and females, separately, underlying

depression (we will call this "depression network"). Fig.2.1 describes the steps involved in forming the ACS and depression networks.

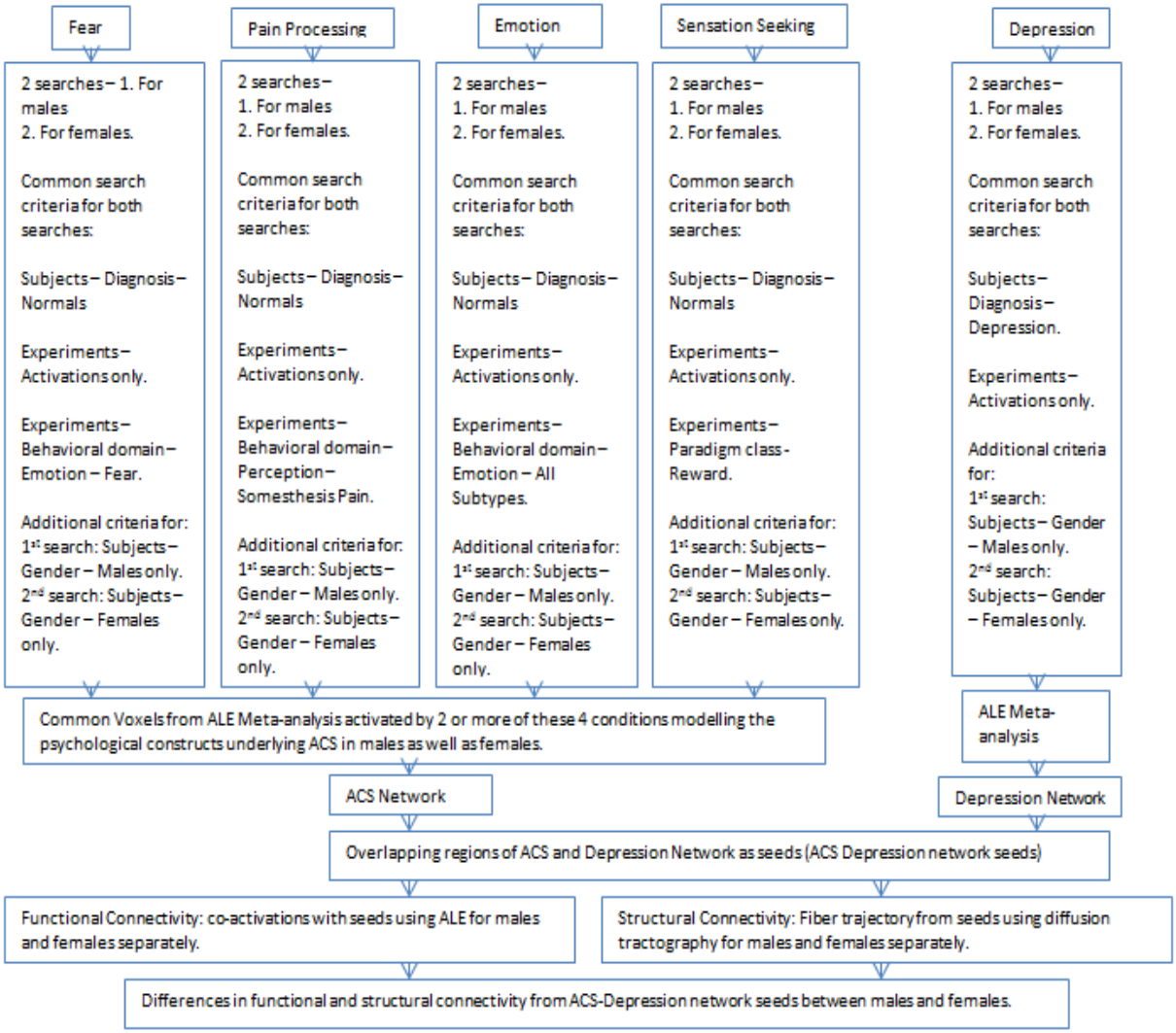

Figure 2.1 *A schematic illustration of the entire procedure involving ALE meta-analysis, meta-analytic functional connectivity modeling and structural connectivity analysis.*

2.2.2 Meta-analytic Connectivity Modeling: An ALE Meta-Analysis

Robinson and colleagues [75] [76] coined the term "meta-analytic connectivity modeling" which is based on the assumption that voxels that are statistically co-activated by a given

condition across many different experiments must be functionally connected [75] [76]. Here, we used this concept to find functional networks underlying ACS and Depression in males and females.

ACS and depression networks were examined to identify overlapping voxels, which may be indicative of common neural substrates underlying ACS and depression in males as well as females. These common voxels (we will call these "ACS-Depression network seeds") were then used as ROIs in a subsequent ALE-based meta-analysis wherein these seed locations were used for obtaining voxels co-activated by them, and hence by inference, functionally connected to them. Further, we investigated whether the functional network obtained by ACS-Depression network seeds using meta-analytic connectivity modeling (we call this "ACS-Depression network") were different in males and females.

2.2.3 Structural Connectivity using Diffusion Tensor Imaging

To investigate the structural basis of the functional networks derived through meta-analysis, diffusion tensor imaging (DTI) techniques were used. White matter axonal tracts, from the ACS-Depression network seed voxels identified previously, were calculated using diffusion weighted data in order to determine the regions structurally connected to them. Diffusion-weighted data were acquired from forty-nine healthy individuals (age: 40.94 years±8.38; education: 12.47 years±2.69; 16 males, 33 females) who were recruited into an Institutional Review Board approved neuroimaging study at the Research Imaging Institute, University of Texas Health Science Center at San Antonio, Texas [76]. All individuals included in the analysis were screened for psychiatric illness and neurological conditions, and had never lost consciousness. Data were acquired on a Siemens 3T scanner with a standard 8-channel head coil. Diffusion weighting was isotropically distributed along 55 directions (b-value=0, 700; repetition time

(TR)/Echo time (TE)=7800/88ms, base resolution=128mm, voxel size=1.72mm × 1.72mm × 3 mm; 50 slices acquired; total scan time=7 min 40 sec). In each subject, a high-resolution T_1-weighted scan was obtained for registration purposes (Magnetization-prepared Rapid Gradient Echo or MPRAGE, TR/TE=2200/3.04ms, flip angle=13°, voxel size=0.8 mm3, 208 slices, base resolution=320 mm, field of view in phase-encoding direction = 70%, field of view in readout direction = 256 mm). All images (diffusion-weighted and T_1-weighted) were skull-stripped using tools provided in FSL software [77], and manually checked to ensure accuracy. Probabilistic diffusion tractography was carried out as described previously [78] [22] [79], using a probability density function that was created at each voxel on the principal fiber direction. Connectivity probabilities were estimated between the seed voxels and target voxels (i.e., the rest of the brain) by repeatedly sampling connected pathways through the probability distribution function. The differences in the white matter pathways originating from ACS-Depression network seeds in males and females were examined. Fig.2.1 illustrates the entire analysis procedure.

2.3 Results

2.3.1 The ACS and Depression Networks

The thresholded ALE maps obtained from conducting ALE meta-analysis on the aforementioned four tenets of ACS: emotional stoicism, pain tolerance, fearlessness about death and sensation seeking were overlaid on the same anatomical image for males and females separately. The regions that were commonly activated by at least two of the four conditions were hypothesized to represent the ACS network for males as well as females (Fig.2.2). Similarly, regions constituting the functional network underlying depression, obtained from ALE based meta-analysis performed for depression are shown in Fig.2.3 for males and females. Table 2.1 provides list of the major regions in the ACS network in males and females, separately showing

regions of overlap as well as gender-specific activations. The regions that were common to the functional networks underlying depression in males and along with those that were specific to males or females are listed in Table 2.2. Note that ALE values are provided in Table 2 and not in Table 2.1 as the latter is an intersection map obtained from four different primary ALE analyses.

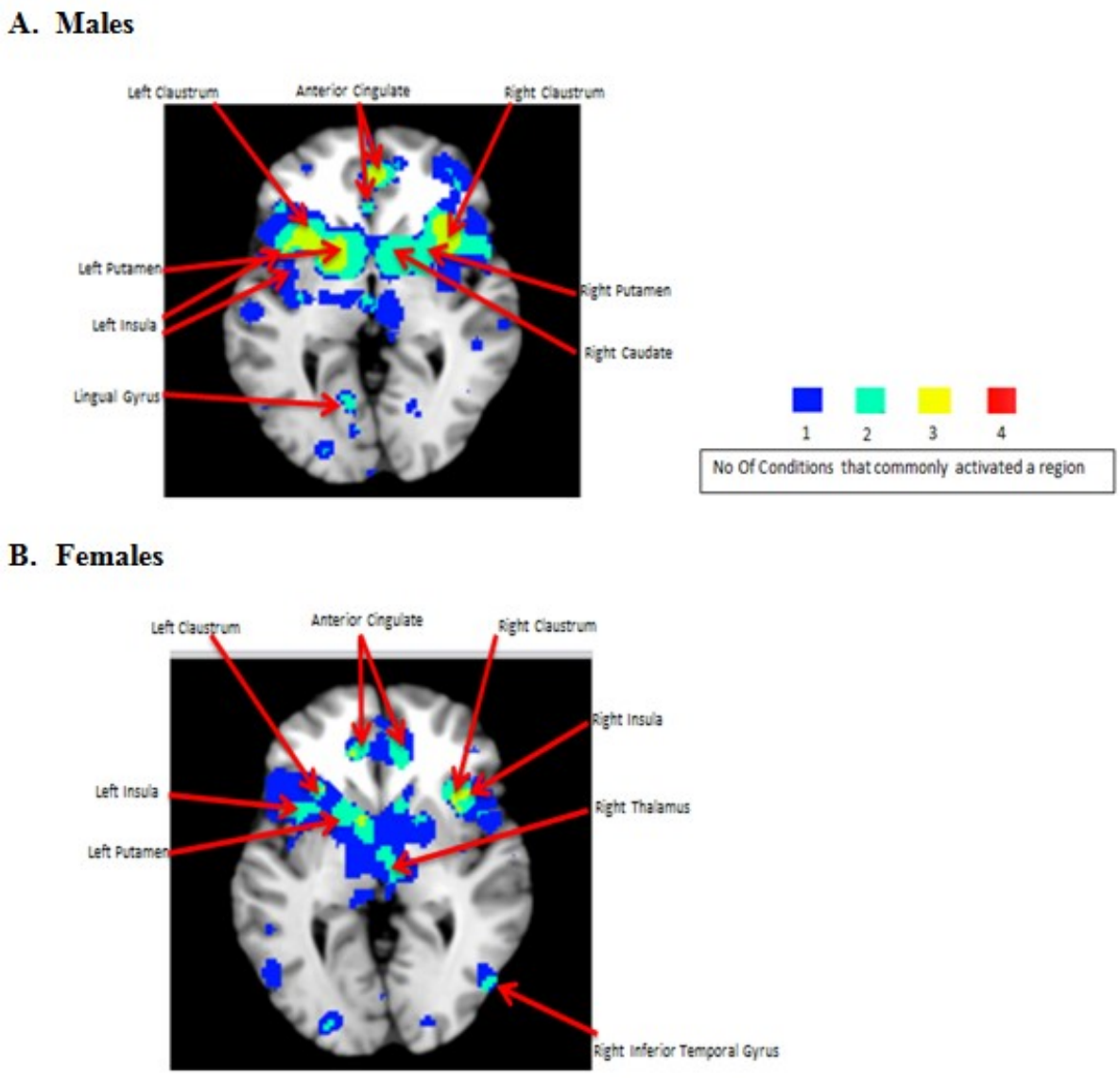

Figure 2.2 *The ACS network for males (A) and females (B). The color bar illustrates the color scheme used for depicting the regions that were commonly activated by just one, two, three or four of the following conditions – emotion, pain processing, sensation seeking and fear. Voxels activated by any one of the above mentioned four conditions are shown in blue, by any two of the above conditions are shown in aquamarine and by any three of the four conditions in yellow,*

respectively. Regions represented by aquamarine and yellow colors together form the ACS network.

Table 2.1 *Activation statistics in males and females corresponding to the ACS network. BA: Brodmann Area*

Lobe	Region	BA	Males			Females		
			x	y	z	x	Y	z
Convergent Seeds								
Sub-lobar	Right Caudate	Caudate Body	8	10	4	8	12	6
	Right Putamen (Lentiform Nucleus)		21	4	4	17	6	6
	Right Claustrum		29	16	4	33	20	3
	Right Insula		41	14	4	36	19	3
	Left Putamen (Lentiform Nucleus)		-18	6	2	-25	-3	-9
	Left Claustrum		-29	17	2	-30	12	6
	Left Insula	13	-40	13	2	-36	11	6
	Right Thalamus		8	2	4	3	-14	2
Male specific network								
Sub-lobar	Left Caudate	Caudate Body		-9			11	2
Frontal	Right Precentral Gyrus	44		48			12	4
	Left Precentral Gyrus	6		-42			0	35
	Right Mid Frontal Gyrus	10,9		35			41	13
				40			17	25
Posterior	Right Cerebellum Declive			33			-71	-17
	Left Cerebellum Declive			-33			-63	-18
Limbic	Right Anterior Cingulate	32		6			45	3

	Right Cingulate Gyrus	23	5	-28	26
Occipital	Right Lingual Gyrus	17	21	-87	8
	Left Lingual Gyrus		11	-63	2

Female specific Network

Sub-Lobar	Left Lat Glob Pallidus (Lentiform Nucleus)		-19	-4	-9
	Amygdala		-20	-7	-13
	Right Lat Glob Pallidus (Lentiform Nucleus)		18	1	-10
Limbic	Left Cingulate Gyrus	32,24	-3	12	42
			-3	9	42
	Left Anterior Cingulate	32	-12	39	0
	Right Anterior Cingulate	24	7	37	4
Parietal	Left Postcentral Gyrus	40	-54	-27	20
Occipital	Right Inf Temporal Gyrus	37	48	-69	2

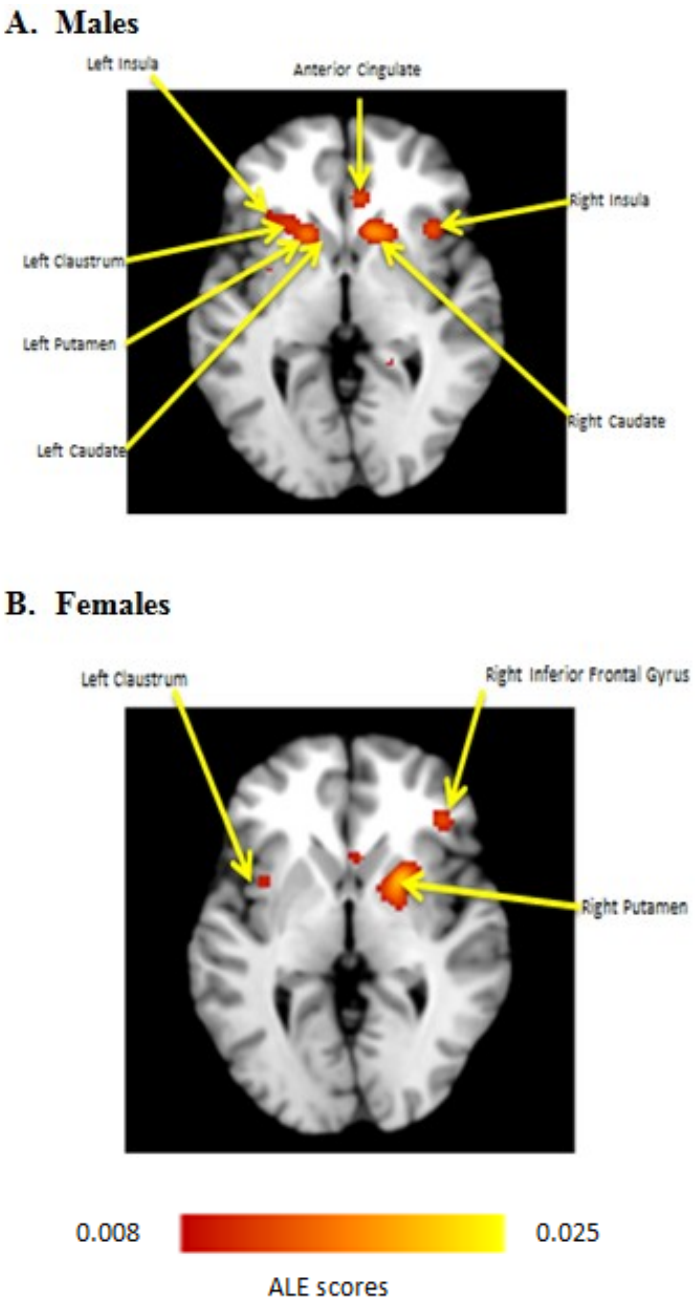

Figure 2.3 *The Depression network for males (A) and females (B)*

Table 2.2 *Activation statistics in males and females corresponding to the Depression network. BA: Brodmann Area*

Lobe	Region	BA	Males			Females			ALE	
			x	y	Z	x	y	Z		
Convergent Regions										
Sub-Lobar	Right Putamen(Lentiform Nucleus)		28	-4	8	22	8	2	0.015	0.020
	Left Putamen(Lentiform Nucleus)		26	-2	8	24	-4	10	0.014	0.024
						22	-2	-6		0.012
						26	10	6		0.009
	Left Claustrum		24	20	4	28	8	-8	0.012	0.014
	Right Insula	13	40	18	16	44	38	18	0.025	0.010
			38	18	4				0.015	
			38	4	10				0.008	
	Left Insula	13	50	18	24	36	6	4	0.012	0.010
	Right Caudate	Caudate Head	14	16	0	2	16	2	0.019	0.009
Limbic	Left Cingulate Gyrus	23	-6	32	28	-8	12	30	0.014	0.013
Female specific Network										
Frontal	Right Inferior Frontal Gyrus	47		40		32		0		0.013
				18		20		-16		0.011
				18		30		-2		0.009
				24		30		-4		0.008
	Left Mid Frontal Gyrus	9		50		14		26		0.010
Limbic	Left Anterior Cingulate	32		-4		20		-8		0.012

	Left Cingulate Gyrus	23	-8	12	30	0.013
	Right Posterior Cingulate	23	4	28	22	0.024
	Right Anterior Cingulate	24,32,25	6	32	4	0.015
			2	26	-8	0.013
			2	2	-4	0.010
	Right Cingulate Gyrus	31,24	12	40	28	0.010
			12	8	26	0.014
	Right Parahippocampal Gyrus	35,36	24	20	-18	0.018
			28	28	-10	0.014
	Left Parahippocampal Gyrus	28,19	20	18	-14	0.013
			24	42	-2	0.010
Temporal	Left Middle Temporal Gyrus	39	44	62	22	0.010
Anterior	Right Cerebellum Anterior Lobe: Dentate		12	52	-22	0.009
Sub-Lobar	Left Lat Glob Pallidus (Lentiform Nucleus)		20	-3	6	
Male specific network						
Frontal	Left Precentral Gyrus	9,6	36	8	38	0.023
			37	5	35	
	Right Precentral Gyrus	6	38	2	34	0.011
	Right Mid Frontal Gyrus	46,8,9	42	28	18	0.014
			28	12	38	0.013
			39	18	23	
	Left Inferior Frontal Gyrus	45	32	24	4	0.010
Parietal	Left Supramarginal Gyrus	40	38	44	34	0.020

	Left Inferior Parietal Lobule	40	46	42	28	0.017
	Right Inferior Parietal Lobule	40	42	34	34	0.015
Sub-Lobar	Left Caudate	Caudate Head	16	16	2	0.016
	Right Caudate	Caudate Body	16	18	26	0.011
	Right Claustrum		36	-4	-4	0.011
	Right Thalamus		4	-4	6	0.011
Temporal	Left Superior Temporal Gyrus	13	36	26	8	0.011
Occipital	Right Lingual Gyrus	30	18	42	0	0.009
Limbic	Right Cingulate Gyrus	23	5	28	28	

2.3.2 The Overlap between ACS and Depression Networks

The voxels identified in the ACS and Depression networks in males and females from Figs 2.2 and 2.3 respectively, were overlaid on a single anatomical image as shown in Fig.2.4 to investigate common neural substrates underlying ACS and depression. The overlap between ACS and Depression networks in males comprised of left precentral gyrus, bilateral putamen, left claustrum, bilateral caudate, right cingulate gyrus, right Insula, right midfrontal gyrus and right thalamus. Likewise, the overlap between ACS and Depression networks in females consisted of bilateral putamen, left lateral globus pallidus and left insula. These activations in the males and females form the ACS-Depression network seeds which were subsequently used in order to determine meta-analytic functional connectivity and DTI-based structural connectivity. As noted before, since the Depression network was assumed to represent a network that may

underlie suicidal desire, the overlap between ACS and Depression networks may form a basis for lethal suicidal behavior. Putamen was commonly activated in ACS-Depression Network in males as well as females. The ACS-Depression network seeds organized by lobes and weighted centers of seeds that were obtained in males and females are enlisted in Table 2.3.

A. **Males**

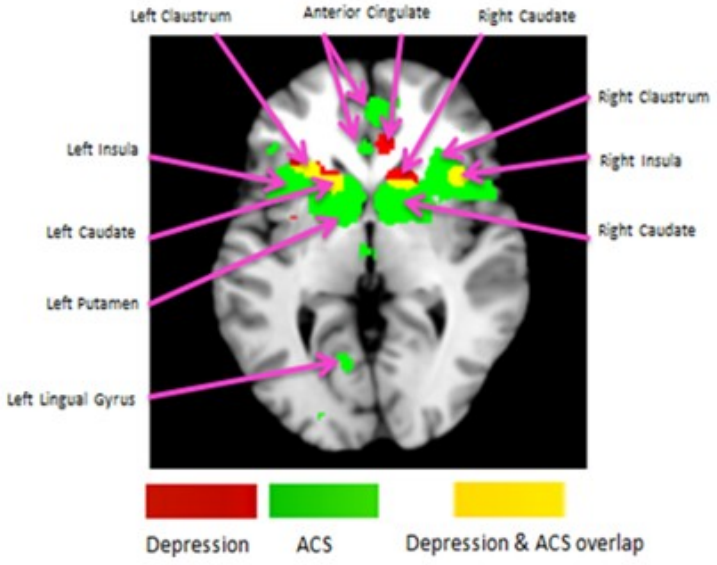

B. **Females**

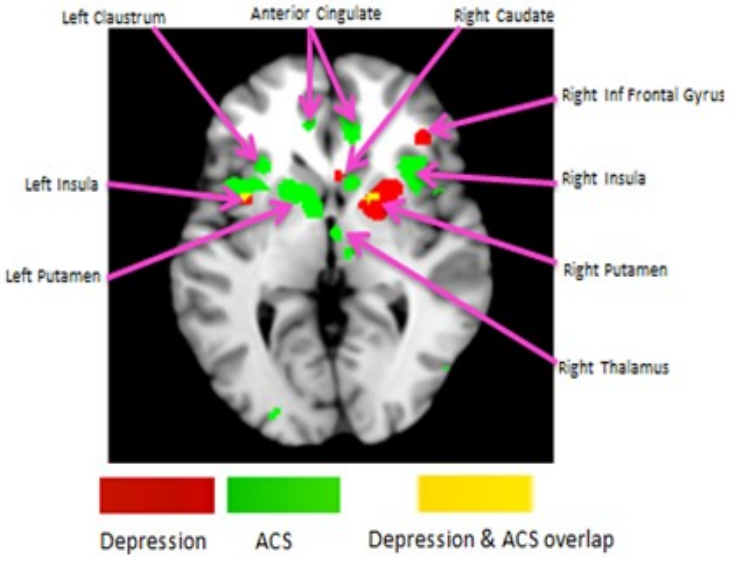

C. **ACS-Depression Network Seeds**

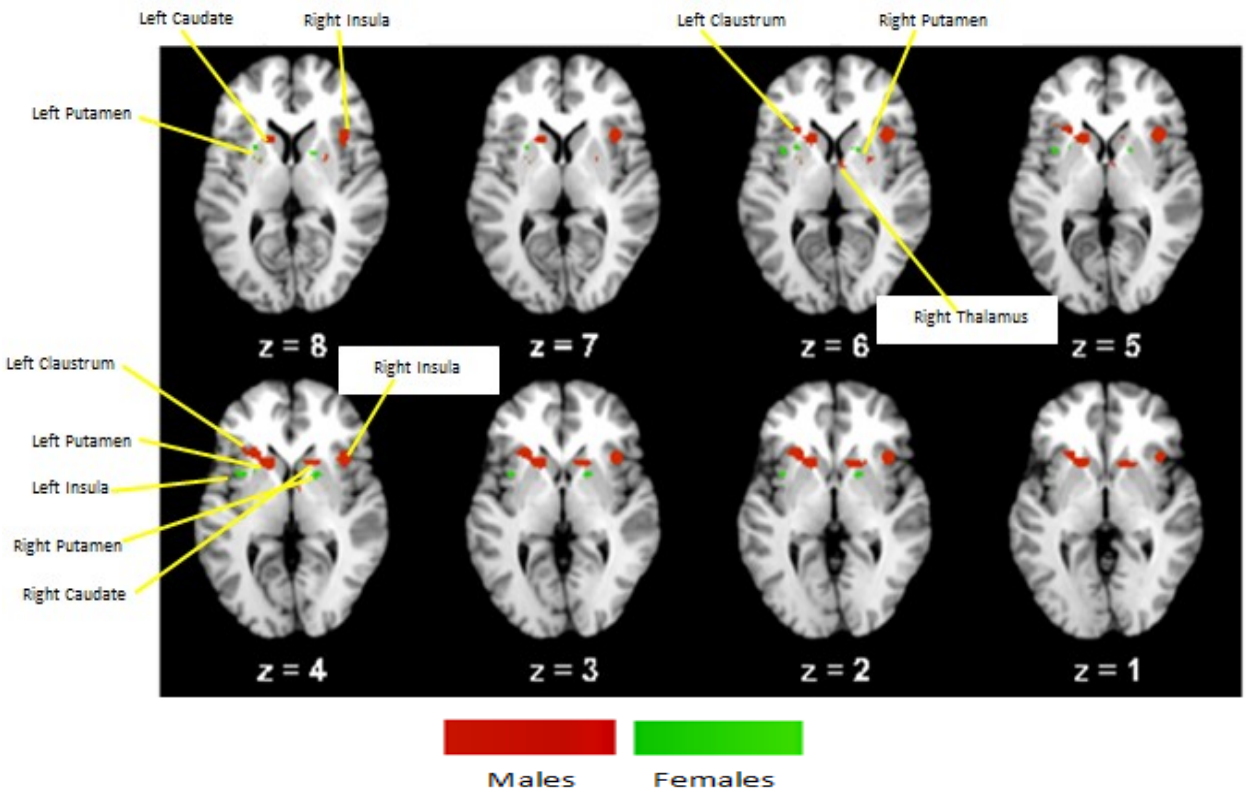

Figure 2.4 ***A:*** *ACS and Depression networks identified in males, both overlaid on same anatomical image.* ***B****: ACS and Depression networks identified in females, both overlaid on same anatomical image.* ***C****: Voxels commonly found in the ACS and Depression networks identified in males and females, overlaid on a single anatomical image. These form the ACS-Depression network seeds.*

Table 2.3 *Seeds corresponding to ACS-Depression network (Fig. 2.4C)*

Lobe	Region	BA	Males			Females		
			x	y	z	x	y	z
Convergent Seeds								
Sub-lobar	Left Putamen (Lentiform Nucleus)		-19	14	4	-26	9	7
	Right Putamen (Lentiform Nucleus)		24	1	7	17	7	4
Female specific Seeds								
Sub-Lobar	Left Insula	13		-37		7		5
	Left Lat Glob Pallidus (Lentiform Nucleus)			-21		0		6
Male specific Seeds								
Sub-lobar	Left Claustrum			-27		21		4
	Left Caudate	Caudate Body		-16		15		4
	Right Caudate	Caudate Body		14		15		4
	Right Insula	13		37		18		5
	Right Thalamus			5		-2		6
Frontal	Left Precentral Gyrus	6		-40		2		35
	Right Middle Frontal Gyrus	9		40		18		23
Limbic	Right Cingulate Gyrus	23		4		-28		28

2.3.3 Functional and Structural Connectivity

We obtained voxels co-activated by the ACS-Depression network seeds (Fig.2.4) separately in males and females using ALE-based meta-analytic connectivity modeling. The corresponding results, shown in Fig.2.5 and Fig.2.6, indicate that even though the ACS-Depression network in males and females underlie a common neurophysiological framework, there are both commonalities and differences in their underlying neural substrates. Major brain regions which were commonly co-activated by the ACS-Depression network seeds in males and females are listed in Table 2.4, while gender specific co-activations are listed in Table 2.5. This provides an exploratory model for differentiating the neural basis of lethal suicide attempts between males and females.

A: Males

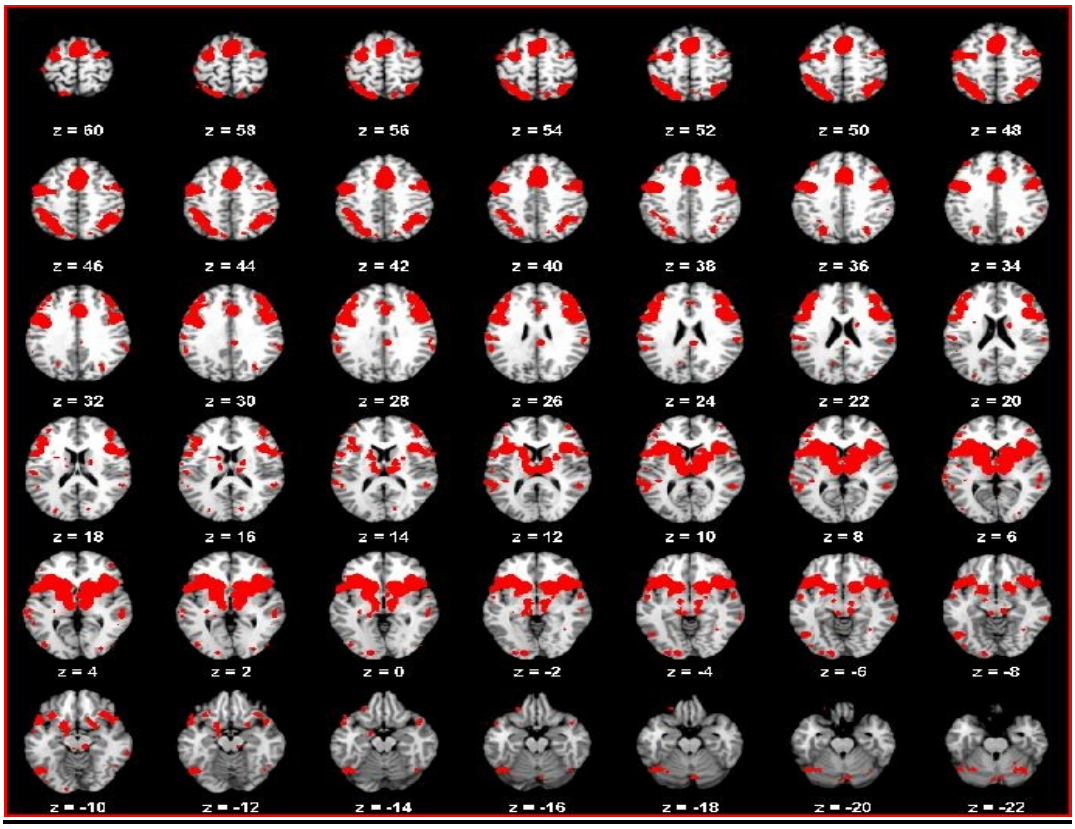

B: Females

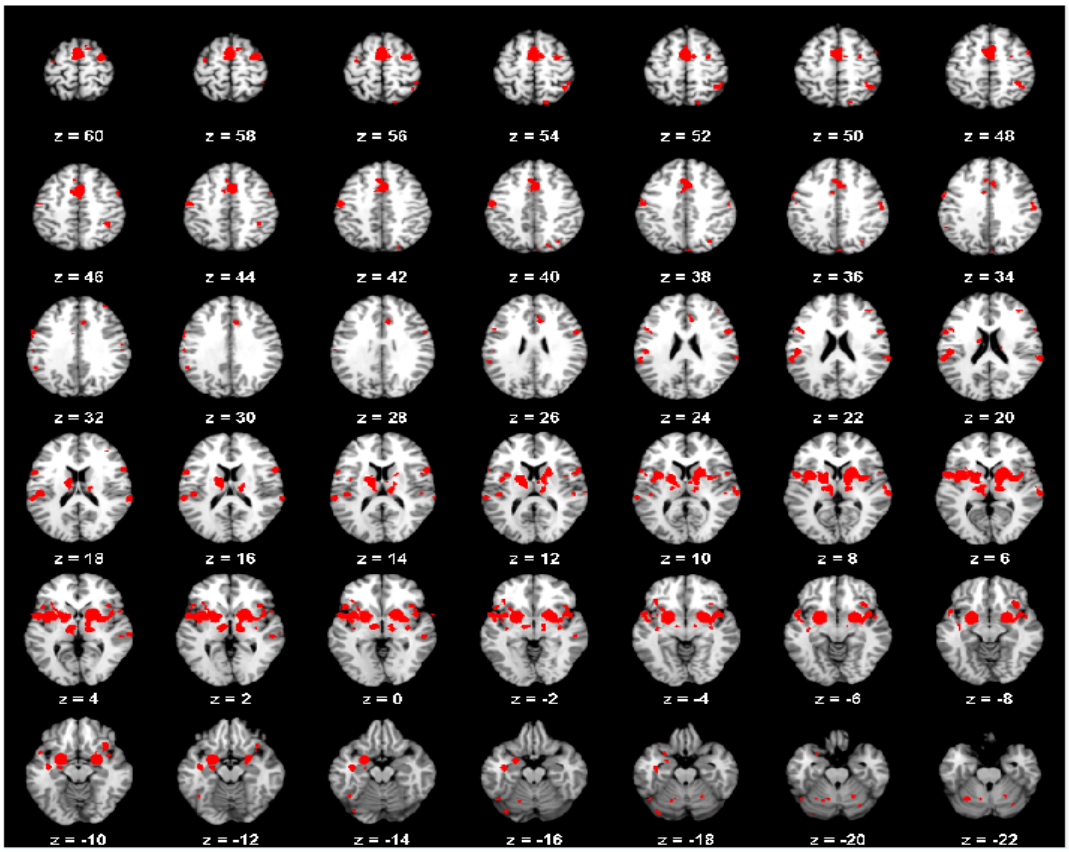

Figure 2.5 *ACS-Depression network in males (A) and females (B) obtained by finding voxels co-activated by the ACS-depression network seeds found in Fig.2.4.*

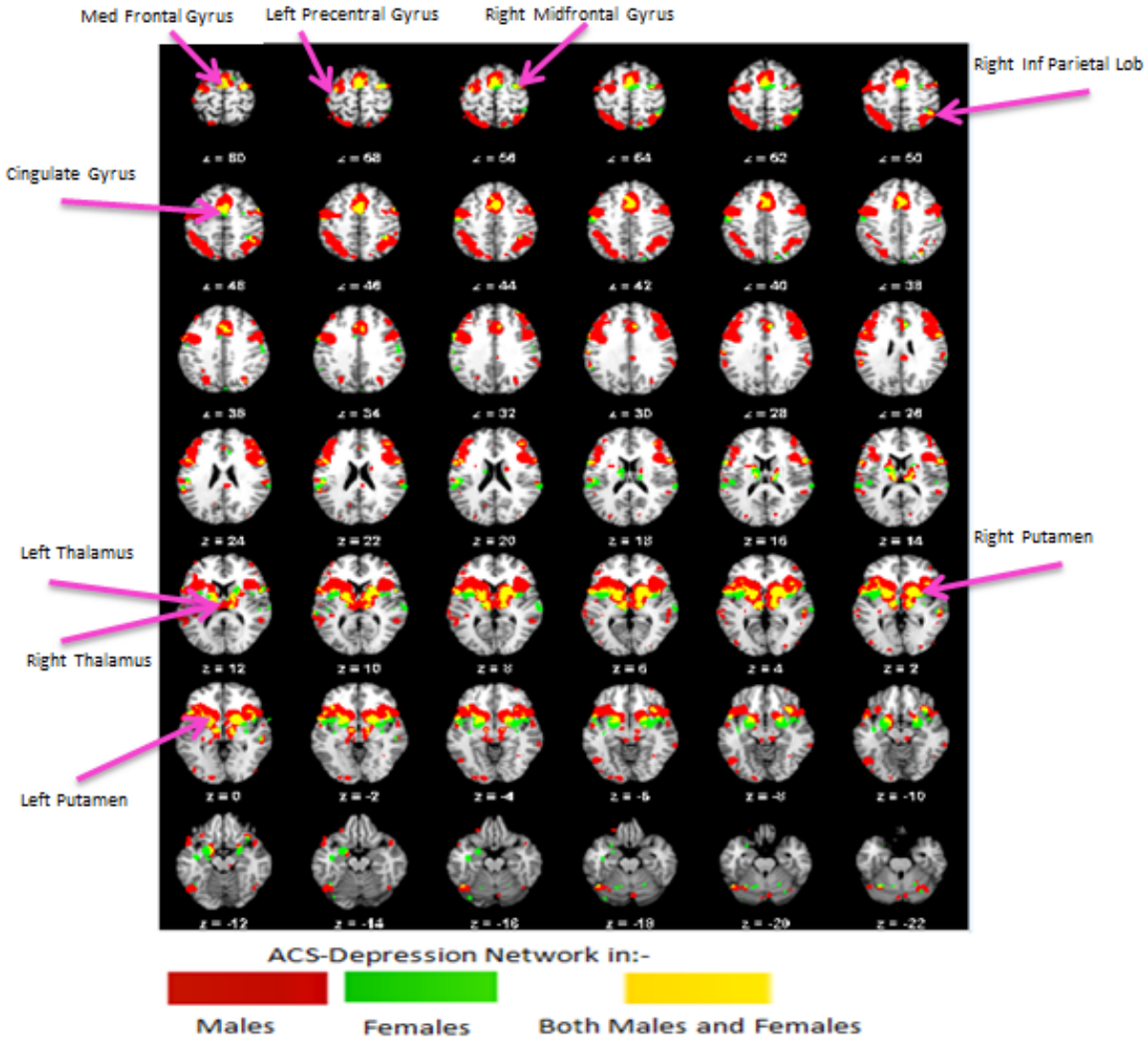

Figure 2.6 *ACS-Depression network, which was obtained separately in males and females, is overlaid on a single anatomical image. Green represents the ACS-Depression network in females, red in males and yellow represents their overlap. Only regions of overlap are labeled in the figure while Table 2.5 provides labels of regions which were exclusively co-activated with ACS-Depression Network seeds only in males and females*

Table 2.4 *Major regions that demonstrated meta-analytic functional connectivity to the ACS-Depression seeds in both males and females*

Lobe	Region	BA	X	y	z
Sub-lobar	Left Putamen (Lentiform Nucleus)		-19	4	4
	Left Lat Glob Pallidus (Lentiform Nucleus)		-19	-3	4
	Left Insula	13	-38	10	4
	Left Thalamus		-10	-16	4
	Right Putamen (Lentiform Nucleus)		23	5	4
	Right Lat Glob Pallidus (Lentiform Nucleus)		18	0	4
	Right Insula	13	42	8	4
	Right Caudate	Caudate Body	13	8	4
	Right Thalamus		15	-15	4
	Right Claustrum		31	24	-7
Frontal	Left Precentral Gyrus	44	-51	8	4
	Left Med Frontal Gyrus	6,32	-3	3	58
			-2	13	43
	Right Med Frontal Gyrus	6,32	4	5	58
			6	15	43
	Right Midfrontal Gyrus	6	28	-3	60
	Right Inf Frontal Gyrus	44	54	11	15
Limbic	Right Cingulate Gyrus	32,24	2	16	41
			2	14	45
	Left Cingulate Gyrus	32,24	-2	23	41
			-3	10	38

Parietal	Right Inf Parietal Lob	40	39	-46	50
Anterior	Left Cerebellum Culmen		-29	-60	-26

Table 2.5 *Male and Female specific major regions exclusively co-activated with ACS-Depression network seeds: Regions that contained some overlapping area between males and females but also were observed to contain some area specific to male/female network are mentioned in red, regions consisting of ACS-Depression seeds are mentioned in violet and regions satisfying both the aforementioned criteria are mentioned in green.*

Male specific regions

Lobe	Regions	BA
Sub-Lobar	Left Claustrum	
	Left Putamen (Lentiform Nucleus)	
	Left Caudate	Caudate Body
	Right Thalamus	
	Right Putamen (Lentiform Nucleus)	
	Right Insula	13
	Right Caudate	Caudate Body
	Left Thalamus	
	Left Insula	13
	Right Caudate	Caudate Head
	Right Claustrum	
Frontal	Left Precentral Gyrus	6
	Right Mid Frontal Gyrus	9
	Left Precentral Gyrus	44
	Left Mid Frontal Gyrus	6,9,46
	Left Inf Frontal Gyrus	9,45,13

	Right Inf Frontal Gyrus	9
	Right Precentral Gyrus	6,9
	Right Med Frontal Gyrus	6,8
	Right Sup Frontal Gyrus 6	
Limbic	Right Cingulate Gyrus	32,24,23
Parietal	Left Inf Parietal Lob	40
	Left Angular Gyrus	39
	Left Precuneus	7,19,39
	Left Sup Parietal Lob	7
	Left Supramarginal Gyrus	40
	Right Sup Parietal Lob	7
	Right Precuneus	7
	Right Inf Parietal Lob	40
Temporal	Left Fusiform Gyrus	37
	Left Sup Temporal Gyrus	22
	Left Mid Temporal Gyrus	21
	Right Sup Temporal Gyrus	41,22
	Right Mid Temporal Gyrus	21
Anterior	Right Cerebellum Culmen	
Posterior	Right Cerebellum Pyramis	
Occipital	Left Mid Occipital Gyrus	37

Female specific regions

Lobe	Regions	BA
Sub-Lobar	Left Putamen (Lentiform Nucleus)	

	Left Lat Glob Pallidus (Lentiform Nucleus)	
	Left Claustrum	
	Right Putamen (Lentiform Nucleus)	
	Right Insula	13
	Right Claustrum	
	Left Insula	13
	Left Thalamus	
	Left Caudate	Caudate Body
Frontal	Left Precentral Gyrus	44
	Right Med Frontal Gyrus	6
	Right Mid Frontal Gyrus	6
Temporal	Right Sup Temporal Gyrus	42
	Right Transverse Tem Gyrus	41

Further we performed axonal fiber tractography using the ACS-Depression network seeds to demonstrate the distinct structural connectivity likely involved in the ACS-Depression network in males and females. The axonal trajectories derived from the ACS-Depression network seeds in males and females are shown in Fig. 2.7.

A: Males

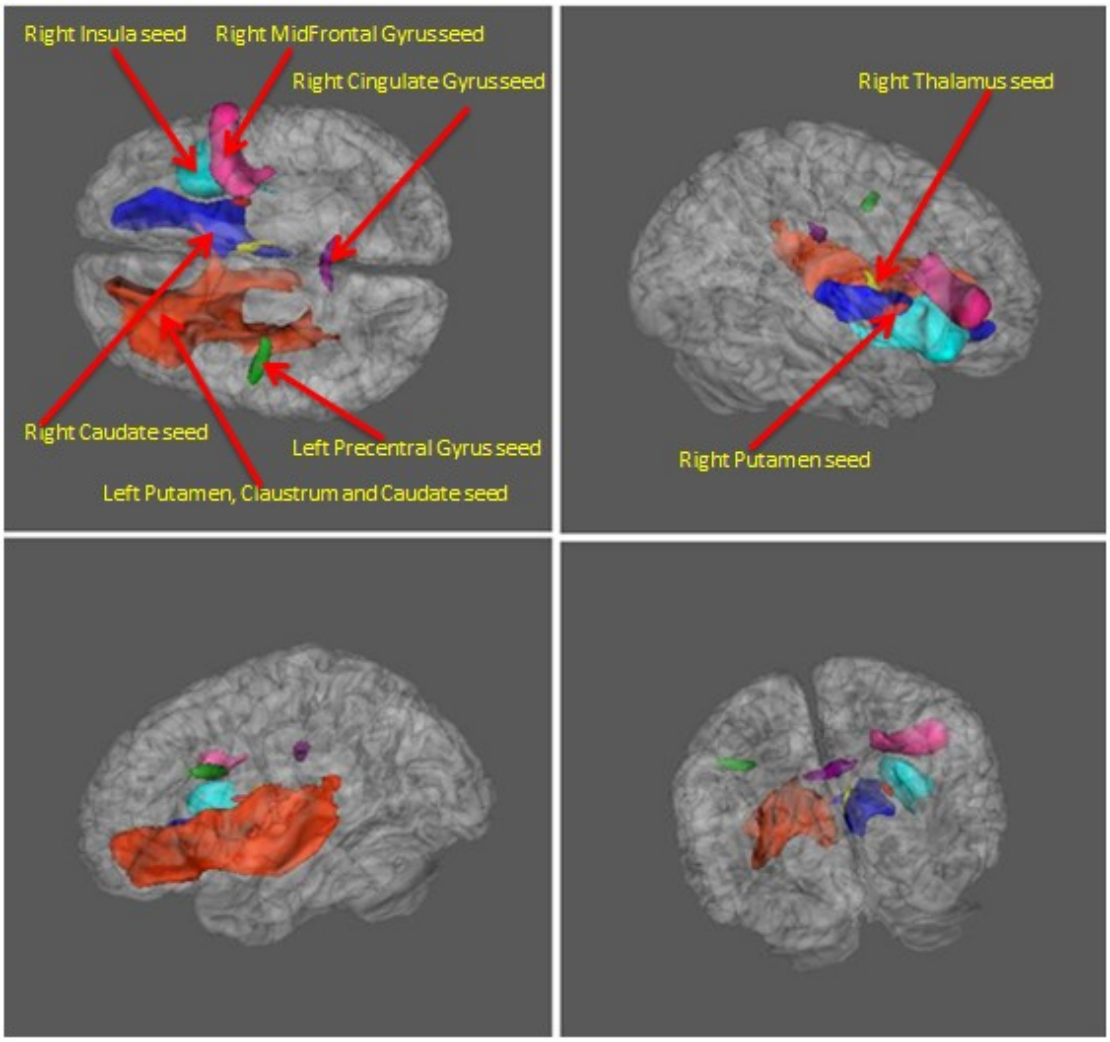
Right Insula seed
Right MidFrontal Gyrus seed
Right Cingulate Gyrus seed
Right Caudate seed
Left Precentral Gyrus seed
Left Putamen, Claustrum and Caudate seed
Right Thalamus seed
Right Putamen seed

B: Females

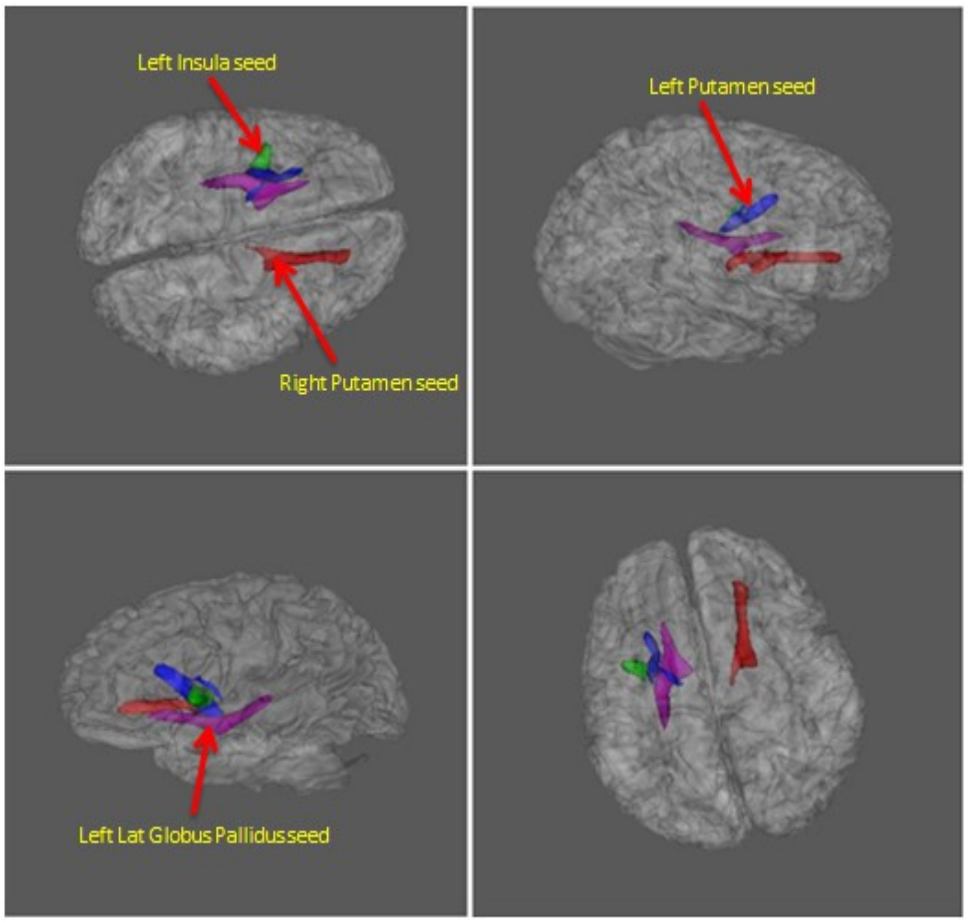

Figure 2.7 *The axonal trajectories derived from the ACS-Depression network seeds defined by co-activated voxels from ACS and Depression networks in males (A) as well as females (B). The four panels in (A) and (B) are the different views of the same figure.* ***A:*** *Yellow – Fibers from Right Thalamus, Green - Fibers from Left Precentral gyrus, Dark Blue - Fibers from Right Caudate, Purple - Fibers from Right Cingulate gyrus, Light blue - Fibers from Right Insula, Pink - Fibers from Right mid frontal gyrus, Red- Fibers from Right Putamen, Orange - Fibers from Left putamen, claustrum, caudate.* ***B:*** *Red - Fibers from Right Putamen, Green - Fibers from Left Insula, Blue - Fibers from Left Putamen, Purple - Fibers from Left Globus Pallidus.*

It can be observed from Fig.2.4, Fig.2.7 and Table. 2.3 that ACS-Depression network seeds in the left and right putamen are present in both males and females. Given the role of putamen in the hate circuit [80] it may mediate gender differences in lethal suicidal behavior (more on this in the discussion). In order to better understand and demonstrate the differences in structural

connectivity between males and females involved in ACS-Depression network, just the fiber trajectories from these seeds in both males and females were overlaid on the same anatomical image in Fig. 2.8. The fiber trajectories from the left putamen seed in males, projected towards left insula, medial frontal gyrus, thalamus and premotor cortex. Whereas in females, the fiber projections from left putamen did not travel farther while that from the right putamen seed projected to the anterior cingulate and thalamus. The structural connectivity analysis depicts that the ACS-Depression network in males might cover a vast expanse of cortical and sub-lobar brain regions compared to females.

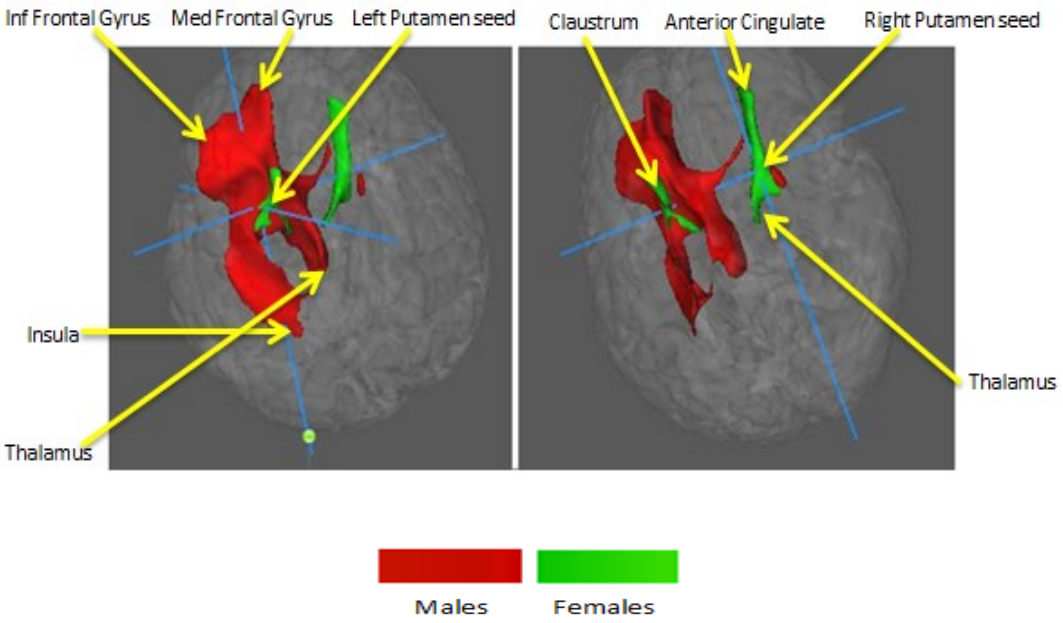

Figure 2.8 *Fibers from seeds in Left and Right Putamen in Males and Females both overlaid on a single anatomical. Red – fibers in males, Green – fibers in females. Both panels represent different views of the same figure.*

2.4 Discussion and Conclusion

One of the most well established findings with regard to suicidal behavior is that men are far likelier to engage in fatal suicidal behavior, whereas women are far likelier to engage in non-fatal

suicidal behavior. Most existing functional and structural studies of suicide are focused on non-fatal suicidal behavior [43]; as such, they do not necessarily provide information about neural substrates involved in fatal suicidal behavior and therefore cannot explain the so-called gender paradox of suicide. The goal of this study was to address this limitation in the literature. Given the challenges inherent in studying the neural basis for fatal suicidal behavior, we used the interpersonal-psychological theory of suicide (IPTS) [51] [52] as a theoretical foundation for identifying potential endophenotypes of fatal suicidal behavior. On the basis of prior research [57], we investigated several psychological constructs relevant to the ACS (i.e., emotional stoicism, sensation seeking, pain tolerance, and fearlessness about death). Gender differences in neural networks that underlie these endophenotypes may eventually help to explain the gender paradox of suicidal behavior. To accomplish our goal, we conducted an exploratory investigation of the neural mechanisms that are differentially activated by the psychological/psychiatric constructs in the ACS and depression in males and females. As noted before, since the Depression network was assumed to represent a network that may underlie suicidal desire, the overlap between ACS and Depression networks may form a basis for lethal suicidal behavior. Here, we have demonstrated that meta-analysis and meta-analytic connectivity modeling can be used to develop neural models and testable hypotheses regarding the gender paradox of suicidal behavior.

Our research has identified a preliminary network of regions commonly activated by two or more psychological constructs underlying the ACS in males and females separately. Given that most functional and effective connectivity models require the definition of *a priori* ROIs, identifying the neural nodes associated with ACS in a sensitive and robust fashion represents a key advancement for future experimental studies that can examine gender differences in the

neural connectivity of these networks. Secondly, we found that the regions corresponding to both the ACS and Depression networks have significantly different foci in males and females, which implies potential for distinct functional and structural connectivity differences. The proportional contribution of each of the regions in the ACS and Depression networks to the individual psychological constructs of the IPTS may provide a gender-specific, multidimensional, imaging biomarker of suicidal behavior. As such, this study provides a foundation for futures studies examining the neural substrates of the ACS, allowing for integration of previous findings of higher male vulnerability for death by suicide and higher female vulnerability for non-fatal suicidal behavior. Importantly, since the ACS is a multidimensional construct, identification of neural regions involved in each of the individual constructs provides the basis for their underlying biosignatures.

2.4.1 ACS Network

Several brain regions demonstrated consistent activation during imaging studies examining psychological constructs thought to be related to the IPTS dimensions. While no previous meta analyses exist that combine all these constructs of the ACS, some studies have reported ALE analyses of individual constructs. For example, a meta-analysis of gender differences in emotional processing has been reported before [81] and is consistent with what we found. There were no regions commonly activated by all four conditions. Fearlessness about death and pain tolerance were not correlated with one another in [57] and thus could be said to develop somewhat independently. Thus, it stands to reason that distinct neural areas might be associated with some of the constructs that contribute to acquired capability

Our data demonstrate that males and females exhibited similar sub-lobar neural network consisting of bilateral putamen, bilateral claustrum, bilateral insula, right caudate and right thalamus identified under two or more of the IPTS dimensions. This network of brain regions represents a sub-lobar nucleus of regions at the crossroads of emotion and cognitive processing, with functional contributions to both systems. Even so, there were notable differences in the functional network identified for males and females. The primary motor cortex and premotor cortex pertaining to bilateral precentral gyrus and right mid frontal gyrus along with regions in cerebellum were activated exclusively in males, whereas females exhibited activations restricted to limbic system regions such as the amygdala and cingulate cortex, commonly known to be involved in emotion formation and processing [82]. The utilization of motor areas in the ACS network in males may imply that if the ACS network is activated in males, there are greater chances of them executing the action as intended, in contrast to females. The inclusion of emotionally reactive regions in the ACS network in females supports suicidal ideation but lack of motor regions engaged in the network might be the reason of females having lower chances of implementing a lethal attempt. Additionally, while males demonstrated bilateral caudate activation, females demonstrated right caudate utilization.

2.4.2 Depression Network.

Several meta-analysis studies have been previously conducted to investigate depression [83] [84] [85] and our results are in general agreement with them. However, to the best of our knowledge, ALE meta analyses on gender differences in depression have not been reported before and hence is a contribution of the present work. In our meta-analysis study, the depression network identified for both males and females comprised of bilateral putamen, left claustrum, bilateral insula, right caudate and left cingulate gyrus. In spite of the commonly activated

regions, depression also exclusively activated some regions specific to either males or females. For males, the caudate that has been known for its involvement in reward processing was identified not only in the right, but also the left hemisphere. For females, we identified the right inferior frontal gyrus, which has been notably linked to depression in several research studies, and serves as a target for transcranial magnetic stimulation [86]. Additionally, females demonstrated activations in numerous regions such as anterior and posterior cingulate cortex which have been implicated to be the neural substrates underlying the vulnerability to suicidal behavior or suicidal ideation [87]. This might explain females being at a higher risk of depression, suicidal ideation and non-lethal suicidal behavior than males.

2.4.3 Neuro-functional Network Supporting Both ACS and Depression.

Regions common to ACS and Depression network were designated as ACS-Depression seeds, separately in males and females. Using meta-analytic connectivity modeling, we obtained regions co-activated by these seeds in males and females, which we designate as the ACS-Depression functional network. Although this network contained some regions that were common to both males and females, there were noteworthy differences in the regions activated in males and females. Such regions (Table. 2.5) were found to contain voxels common to both males and females but also had voxels which were exclusive to the male or female networks. This indicates some level of functional parcellation/differentiation in these brain regions. The notable amount of premotor, primary motor and cerebellar regions engaged in the ACS-Depression network in males might point towards the existence of a neural substrate supporting motor action. This could possibly result in higher probability of a fatal outcome in men on account of experiencing suicidal desire compared to women. Males also engaged a larger ACS-

Depression functional network than women, which might be a factor responsible for higher lethal suicidal behavior in men.

2.4.4 Structural Network for ACS-Depression

The putamen was the only brain region commonly present in the ACS-Depression network seeds for males and females. Therefore, this may be a region of particular importance in understanding suicidal behavior across men and women. This result is consistent with a recent meta-analytic finding that individuals with a history of suicidal behavior had decreased volumes in the putamen compared to individuals with a history of psychiatric disorders [87]. Upon investigation of the fiber trajectories from the putamen seeds in males and females, differential structural connectivity patterns were observed between males and females. The trajectories from the left putamen seed in males projected up to the premotor cortex, medial frontal gyrus, left insula and thalamus. Premotor cortex (involved in motor planning), medial frontal gyrus (known to play a role in executive mechanisms [88]) and left insula have been previously shown to form a part of the hate circuit [80] that is engaged while experiencing hate towards an individual, which may be relevant to self-hatred. Engaging a large portion of hate circuit and more importantly direct structural connections amongst the regions in the hate circuit might strengthen the intent of suicide and its execution in males, especially given the involvement of the premotor cortex. While the projections from the left putamen in females were localized, females had projections from the right putamen seed extending up to the anterior cingulate and thalamus. The anterior cingulate has been implicated in a previous study [87] to be a neural substrate underlying suicidal ideation. This might be a reason for higher vulnerability of women for suicidal ideation and non-fatal attempts. The regions identified in the functional ACS-Depression

network and the structural connectivity of the ACS-Depression seeds may be the key to understanding gender differences in the rates of fatal and non-fatal suicidal behavior.

The results of this study have important implications for the construct validity of ACS. The vast majority of research on ACS has utilized either self-report measures or assessments of physical pain tolerance; to our knowledge, this is the first investigation of neural substrates that may underlie ACS. By constructing a layout of the neural networks, research will also be enhanced as efforts are directed toward answering more complex questions about how neuronal networks contribute to suicidal behavior.

2.5 Limitations

Some limitations of the current study are noteworthy. First, and perhaps most importantly, we did not investigate suicidal behavior as an outcome variable. Thus, future research is needed to demonstrate a link between the proposed ACS network and fatal suicide attempts as an outcome. Second, there are few imaging studies investigating the specific constructs of ACS, i.e. emotional stoicism, sensation seeking, pain tolerance, and fearlessness of death. Therefore, we performed meta-analyses on emotion, reward, pain, and fear, respectively (since they represent a super-set of the original constructs of ACS), with the assumption that the voxels activated in more than two of the four conditions would be related to ACS. This illustrates one of the weaknesses of meta-analyses. Nevertheless, it is useful to make this assumption as an attempt to generate a hypothesis about the underlying neural substrates of ACS so that future experimental studies may perform experiments to confirm or deny the hypotheses generated by this initial attempt. Similarly, our definition of the ACS network is not ideal (i.e., greater than 2 of the IPTS dimensions), and as the databases become larger, we may be able to refine this definition. Third, we did not investigate all components of the IPTS. Thus, although our results demonstrate that

the ACS network is distinct from the depression network, future research is needed to investigate whether distinct neural substrates underlie ACS versus thwarted belongingness and perceived burdensomeness. Fourth, deactivations were not considered in these meta-analyses for the following reasons: a) deactivations are not as frequently reported as activations, and b) the neural basis of fMRI-based deactivation is yet unclear, i.e. there is still a debate whether deactivations in fMRI are indeed caused by GABAergic inhibition [89] [90]. Finally, the limitations of ALE-based meta-analysis, which have been discussed before, also apply to this study [91] [75] [76] [26]. Despite these limitations, this study provides a useful foundation for future studies of gender differences in the neural basis of suicidal behavior.

Chapter 3: Characterization of Structural Connectivity of the Default Mode Network in Dogs using Diffusion Tensor Imaging

My contribution to this study was creating tensor-based atlas for canine model, performing tractography, generating and compiling the results and writing the entire description. I would like to acknowledge Dr. Robinson for guiding me through the tractography technique and Dr. Deshpande for overall guidance regarding the idea as well as writing the description of the study. I also acknowledge Dr. Salibi, Dr. Beyers & Dr. Denney for contributing the DTI data acquisition, and Dr. Waggoner, Dr. Morrison & Dr. Vodyanoy for their contribution towards canine handling, canine physiology and experimental design.

Abstract

Diffusion tensor imaging (DTI) provides us an insight into the micro-architecture of white matter tracts in the brain. This method has proved promising in understanding and investigating the neuronal tracts and structural connectivity between the brain regions in primates as well as rodents. Canines being cognitively higher than rodents but not as advanced as primates, fit somewhere in the middle of the evolutionary ladder rendering them quite useful to be used as animal models in translational research. In this study, we acquired diffusion data from anaesthetized dogs and created a DTI-based atlas for a canine model which could be used to investigate various white matter diseases. We illustrate the application of this atlas by calculating DTI tractography based structural connectivity between the anterior cingulate cortex (ACC) and posterior cingulate cortex (PCC) regions of the default mode network (DMN) was investigated in dogs. The white matter connectivity was investigated to provide structural basis for the dissociation of anterior and posterior parts of DMN found in a recently conducted resting state fMRI study. A comparison of the integrity of long range structural connections (such as in the

DMN) between dogs and humans is likely to provide us with new perspectives on the neural basis of evolution of cognitive functions across the evolutionary hierarchy.

3.1 Introduction

Diffusion tensor imaging (DTI) is a magnetic resonance imaging technique that measures the anisotropic diffusion of water molecules in tissues providing useful structural information about white matter and indicating the orientation of neural tracts. DTI first came into existence in the mid-1980s [92] [93] [94] and has been rapidly developing ever since. This technique is noninvasive and is now widely used for studying structural connectivity in healthy populations as well as in psychiatric and neurological diseases traditionally characterized by white matter deficits. Researchers have been using DTI to study human and monkey brains and more recently, to study rodent brains such as mice [95]. However, there have been only a handful of studies applying this powerful method to canines, despite the increased use of these animals in research [96] [97]. . In the evolution hierarchy,canines take a position in the intermediate rung on the evolutionary ladder above rodents such as rats, and below cognitively developed species such as monkeys and humans. . Studying the canine model might thus give us a perspective into the evolution of cognitive functions in the upper stages of the evolutionary hierarchy. Additionally, dogs serve as a large animal model, critical for translation of quantitative MRI methods to clinical populations [98], share common environment with their owners until their old age, and receive a good level of healthcare [99]. Furthermore, Rabies has a long history of association with dogs and is almost never known to infect or to be transmitted to humans by small rodents such as rats, chipmunks or rabbits [100]. Dogs also display joint attention with humans and respond to human pointing and gesturing making them an excellent animal model for human

social cognition [101] [102] [103] [104]. This makes them an interesting species worth studying as animal models in translational research to study aging and its effect on disease progression as well as to investigate human diseases that affect white matter integrity such as neurological demyelinating conditions (e.g., Multiple Sclerosis) [98] , GM1 gangliosidosis, a fatal neurodegenerative lysosomal storage disease [105] and Rabies, a virtually incurable disease [106]. Thus non-invasive imaging of neural white matter tracts in the dog brain by using DTI could prove to be very useful.

There have been a few DTI studies conducted on canine models including an *ex-vivo* study that was conducted on euthanized canine brains to study the white matter fibers by analyzing the fractional anisotropy (FA) and directional maps computed using the DTI images acquired within first 2 hours after death [96] and an *in vivo* study investigating feasibility of diffusion tensor tractography in a canine model for studying the cerebral white matter in dogs [97]. However, to our knowledge, ours is the first study to date, to have investigated *in vivo* diffusion images of dog brains to provide us with group-wise FA color maps. Therefore in this study, we aimed to build a canine DTI-atlas, and demonstrate the utility of the atlas by testing a hypothesis derived from previous work in our lab [107] .

With regard to the second aim of our study based upon a resting state fMRI study recently conducted on dog brains in our lab [107], we aspired to test the hypothesis that the functional connectivity dissociation between the anterior and posterior parts of the DMN in the canine model possesses a structural basis.

To accomplish the aims of our study, we first acquired diffusion-weighted images (DWI) in anesthetized dogs to develop a DTI-based atlas of the dog brain for use in future studies by giving an insight into the structural connectivity inside the dog brain. Second, we illustrate the

utility of the dog DTI atlas to test a specific hypothesis arising from our previous resting state functional magnetic resonance imaging (fMRI) study as mentioned previously [107]. Specifically, in our previous study we observed that the anterior and posterior parts of the default mode network (DMN) seem to be dissociated, unlike in monkey and human brains [108] [109]. Therefore, we hypothesized that DTI tractography could provide a structural basis for this dissociation in the form of weaker structural connection between these regions in dogs as compared to humans.

The DMN is an interconnected network of brain regions that is active when an individual is at rest and becomes less active when performing attentionally demanding tasks [110] [111] The network preferentially activates when an individual is daydreaming, engaged in self-retrospection and self-introspection [112]. The core brain regions of DMN, consist of the medial prefrontal cortex (MPFC), posterior cingulate cortex (PCC), inferior parietal cortex (IPC), inferior temporal cortex (ITC) and (para) hippocampal formation. The main hubs of the DMN are within the MPFC and along the posterior midline including PCC [112]. In DMN, PCC has been proposed to be of special interest as it is the only region that directly interacts with all other DMN nodes [113].The anterior regions (ACC/MPFC) upon interacting with medial temporal lobe, facilitates flexible use of the episodic memories and associations to construct self-relevant mental simulations and has also been implicated in judgment of others [114]. Above mentioned two subsystems converge on important nodes of integration including PCC. PCC is commonly associated with episodic memory retrieval [115] [116]. Therefore, DMN is believed to be responsible for consciousness and self-referential processing and has been linked to human cognition [112] [117] [118]. Studies have demonstrated the existence of DMN in humans and monkeys [108] [109], however there are conflicting reports on whether they exist in rodents

[119] [120] [121]. Our resting state fMRI study conducted on dog brains indicated that the anterior and posterior parts of the DMN are dissociated in dogs [107]. Previously conducted research has illustrated that the DMN exhibits highest overlap in its structural and functional connectivity [122]. Therefore, we believed that there might be a significant possibility of the existence of a structural basis for the observed dissociation in the DMN in dogs. We thus decided to investigate it in the anticipation of attaining an insight into the evolution of cognitive functions across the evolutionary ladder.

3.2 Methods

All methods and experiments were approved by the Auburn University Institutional Animal Care and Use Committee. DWI data were acquired using a 3T MAGNETOM Verio (Siemens Healthcare, Erlangen, Germany) MRI scanner from 23 anaesthetized Labrador retriever dogs using a human knee coil (serving as a dog head coil) and an EPI (Echo Planar Imaging) based diffusion sequence with the following parameters: TR=3.6 s, TE=95 ms, flip angle=90˚, 128×128 acquisition matrix, 30 diffusion directions, b=0 and 1000, voxel size=3×3×3 mm^3. Dogs were sedated and lightly anesthetized with intramuscularly administered xylazine (2.2 mg/kg) and ketamine HCL (11 mg/kg,), respectively. Data were preprocessed using the standard FMRIB's Diffusion Toolbox (FDT, which is part of the FMRIB software library (FSL) [123] [124] [125] . Data were first brain extracted, and then corrected for eddy current induced distortions.

3.2.1 DTI-based Atlas

Following eddy current correction **[126]**, diffusion tensors were fit to the corrected data, creating tensor and fractional anisotropy (FA) maps for each dog **[123]**. Individual FA maps were then registered to a high-resolution canine *ex vivo* template created in a previous study **[127]** using FMRIB's linear registration tool (FLIRT) **[128] [129] [130]**. The resulting transformation matrix, computed while registering FA maps to the template, was applied to the tensor maps for each dog, thus obtaining the vector data of each subject in the same standard space using the "vecreg" command line tool in FSL as described in **[131]**. By averaging FA maps as well as vector data in the template space for all the dogs, an average FA map and average color-coded tensor map were computed to reduce the inter-subject variability in canine brain.

3.2.2 Diffusion Tractography

Diffusion parameters were modeled using the BEDPOSTX tool in FSL for the eddy corrected data, and then probabilistic tractography was implemented as described previously [78] [22] [79] using the PROBTRACKX tool in FSL to estimate the likely connections between two regions of interest (ROIs). The ROIs were defined as 4mm radius spheres in the posterior cingulate cortex (PCC) and in the anterior cingulate cortex (ACC). Probabilistic tracking was achieved by a creating probability density function at each voxel on the principal diffusion directions. Connectivity probabilities were estimated between the ROIs by repetitive sampling of the streamlines through the probability distribution function. The ROIs were registered to each subject using the inverse of the previously computed transformation matrix. In this way, fiber tracts were calculated in the subject space, and then transformed to the template space by applying the appropriate transformation computed earlier. ACC-PCC tracts of each subject were

then binarized and compiled to create a group level probability map of the tracts for dogs with a subject count threshold in which the value of each voxel represents the number of subjects that had a tract passing though that voxel. The group level probability map of the ACC-PCC tracts was binarized and overlaid on the group-wise mean FA map computed earlier. A group-wise mean FA value was extracted from the ACC-PCC tracts by averaging the FA values for the voxels constituting the ACC-PCC group-level connectivity map.

3.3 Results

Average FA and tensor-based maps computed for individual dogs using the diffusion tensor computed from the acquired DWI data (Fig 3.1A), and a group-wise average FA map with associated color map representing the first principal vector (i.e., the main diffusion direction) are shown in Fig. 3.1B. This provides a robust atlas void of disproportionate influence from any one subject. Fractional anisotropy values in the group FA map ranged from 0 to 1, with values closer to 1 in regions with higher anisotropy and more directional diffusion of water such as white matter, and closer to 0 in the areas of the brain with isotropic diffusion such as cerebrospinal fluid (CSF). Group mean FA was extracted from the ACC-PCC tract which was found to be 0.32 which is much lower compared to the mean FA previously calculated for humans (young adults) [132], which was 0.57 (the caveats associated with this comparison are discussed in the next section). Additionally, the group level probability map of the tracts is shown in Fig 3.2. The map shows the number of dogs having a tract passing through each voxel. Tracts connecting ACC to PCC were detected in only 9 out of 23 dogs. Even though, the tracts were detected in 9 of 23 dogs, the probability maps show voxel values less than 9 due to the inter-subject variability in the precise fiber pathways from one voxel to the next.

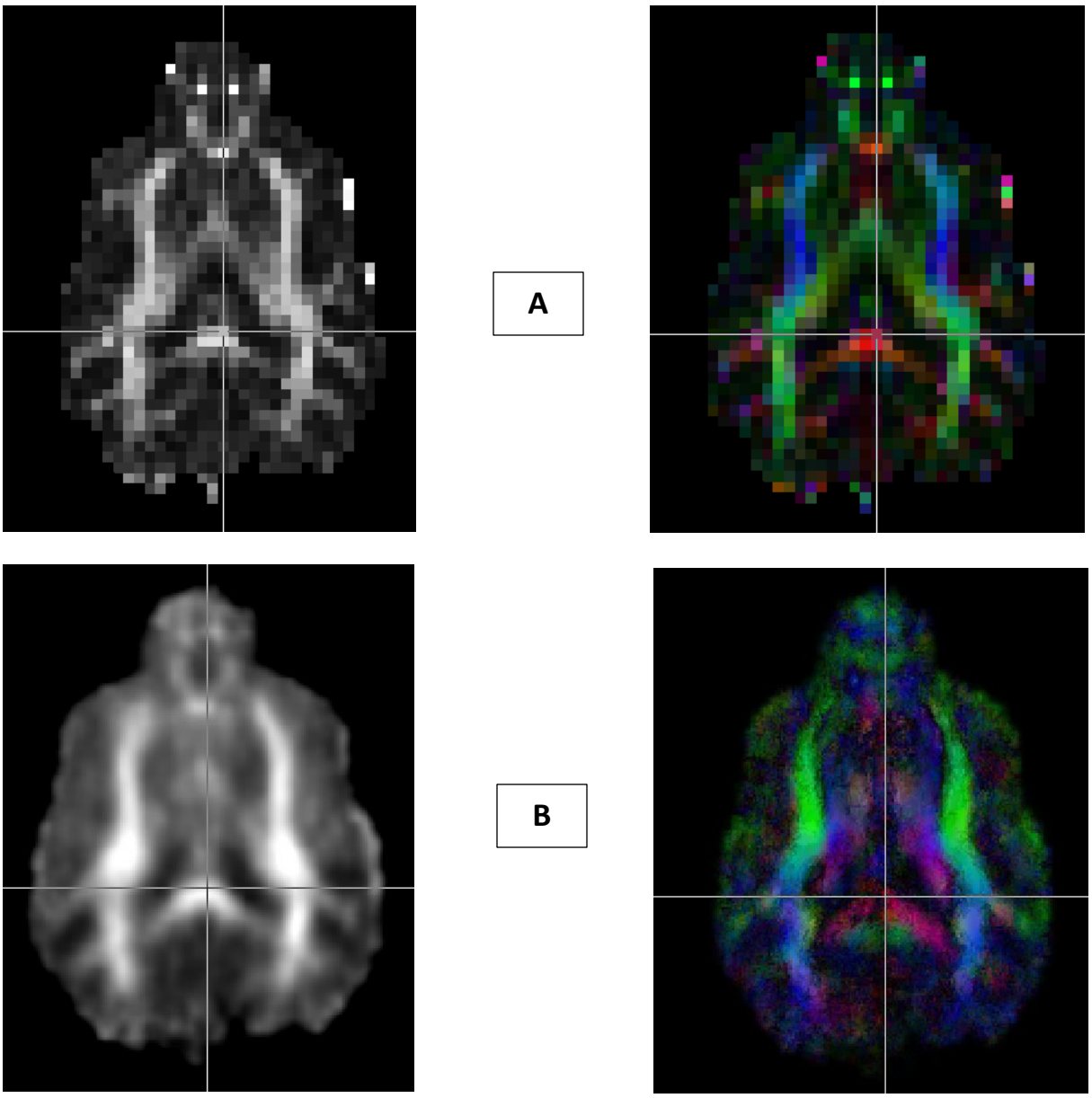

Figure 3.1. ***A:*** *FA map and Tensor based color map for one individual dog.* ***B:*** *Average FA map and color map atlas using a group of 23 dogs. Color map represents left-right tracts in Red, anterior-posterior in Green and superior-inferior in Blue.*

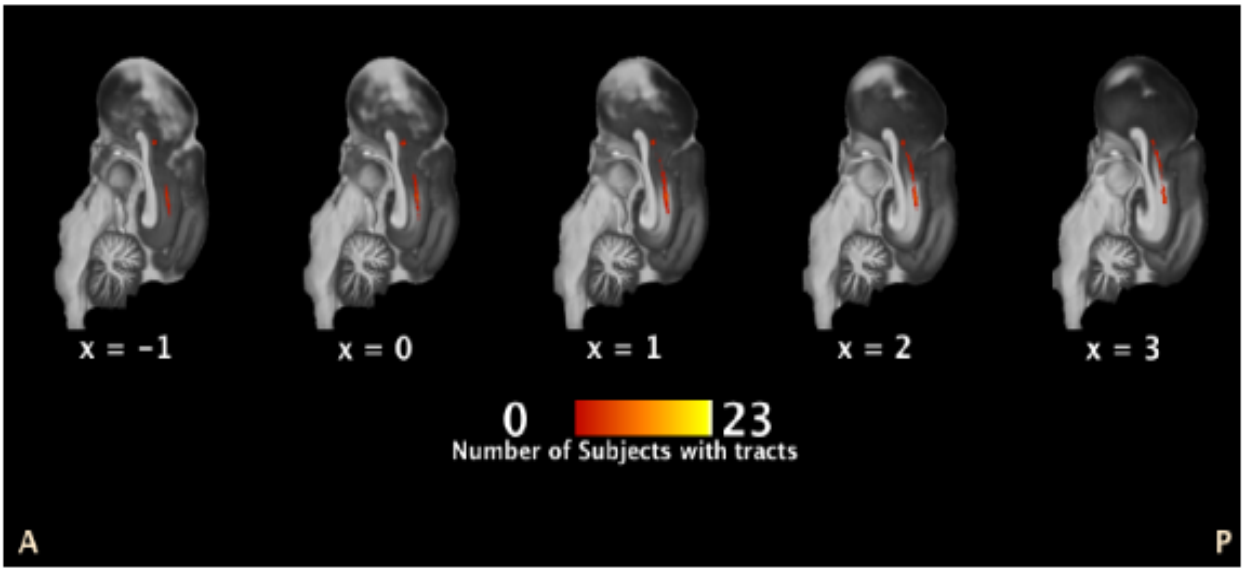

Figure 3.2. *Group level probabilistic map of ACC-PCC tracts. The color scale indicates number of subjects that had a tract in a given voxel.*

3.4 Discussion and Conclusion

The average color map gives a qualitative characterization of the neural tracts in the white matter of a canine brain. The group-wise average FA map and tensor based map provides us with a DTI-based atlas for dogs by accounting for the inter-subject variability. This atlas can be utilized in future studies in both veterinary medicine and translational research.

As previously discussed, studying canines as animal models in translational research could prove promising, keeping in mind that canines lie at an intermediate stage between primitive species (e.g., rodents) and highly advanced species (e.g., primates) in the evolution hierarchy. Further, given their co-evolution with humans [101] [103]and capabilities such as joint attention [133] [104] [102], they are an interesting species worth studying to investigate the cognitive evolution (especially social cognition) in humans. One brain network that has been implicated in cognition in general (as well as in social cognition) [134] [135] is the default mode network. It is

also known to underlie self-referential processing, consciousness, self-awareness and higher cognition in humans [112] [117] [118].

A previous resting state fMRI study investigating the existence of DMN in dogs, demonstrated disconnected ACC and PCC, the anterior and posterior regions of DMN [107]. There is evidence that suggests that DMN has strong correlation between its structural and functional connectivity [122]. Therefore, in this study we tested the hypothesis that the functional finding about the anterior-posterior dissociation of the DMN in canines possesses a structural basis. The group mean FA for the ACC-PCC tracts identified in the dog brain was notably low and also comparably lower than that observed in humans [132]. Additionally, a maximum of only 9 dogs out of 23 had the same tract which indicates significant individual variability in the ACC-PCC tracts. As previously reported in a study conducted with humans [136], tracts connecting MPFC/ACC to PCC were detected in 22 of 23 subjects. Low FA values in ACC-PCC tracts in dogs leading to probable less number of fibers might have contributed to increased individual variability. This finding, although not statistically characterized, seems to lend support for our hypothesis that the weaker resting state functional connectivity found between ACC and PCC in dogs compared to humans may have a structural basis. This might also suggest that evolution of higher cognitive functions in humans is supported by stronger functional and structural connectivity between anterior and posterior regions of the DMN.

3.5 Limitations

While creating a DTI atlas for the dog brain is a clear contribution of the paper, direct comparison of FA values between dogs and humans for testing our specific structural hypothesis regarding the DMN involves certain caveats: (i) the size of the brain in dogs is smaller than in

humans, but the spatial resolution of diffusion data acquired was not proportionally higher in dogs, (ii) the exact placement of seed ROIs in humans is likely to be more accurate than in dogs given that labeled atlases are available in humans, (iii) the anatomy of dog and human brains, especially the frontal cortex, may not be exactly comparable, and (iv) we have assumed in this study that low FA values in the ACC-PCC region in dogs might suggest probable less number of fibers. However, FA values can be influenced by a number reasons such as density of fiber tracts or integrity of the tracts. FA values measure the degree of anisotropy or directionality of diffusion of water molecules along different axes. Thus it is only an indirect measure and not an accurate measure of fiber density. Notwithstanding these limitations, our preliminary results regarding the anterior-posterior structural (as well as functional) dissociation in the canine DMN is worth exploration in the future for understanding the evolutionary significance of the DMN as well as for understanding the position of dogs in the evolutionary hierarchy.

Acknowledgment

Funding from Auburn University's Intramural Grant and from the Defense Advanced Research Projects Agency (government contract/grant number W911QX-13-C-0123) is gratefully acknowledged

Chapter 4: Conclusion

The aim of this thesis was to investigate brain function and structure given their close relationship, by utilizing the non-invasive techniques of functional MRI-based meta-analysis and diffusion tensor imaging. In this thesis, two major research issues were explored: (i) the gender paradox in fatal as well as non-fatal suicidal behavior as most prior studies have mainly aimed towards investigating non-fatal suicide. (ii) the possibility of structural basis to the previously found anterior-posterior dissociation in the Default Mode Network (DMN) in dogs in a resting state fMRI study as well as voxel-specific atlas of tensor (and hence, axonal) orientations by adapting existing human pipelines to canine model.

Suicidal death being a growing problem in today's society, especially amongst men has led to an urgent need to investigate the neural substrates distinguishing fatal and non-fatal suicidal behavior and explaining the gender differences. Therefore, first goal of this thesis was to identify neural networks underlying fatal suicidal behavior and gender differences in both fatal and non-fatal suicidal behavior in an attempt to form specific new hypotheses which can be tested in future experimental studies. To accomplish this goal, we conducted an exploratory investigation of the neural substrates underlying the psychological constructs in the ACS (i.e., emotional stoicism, sensation seeking, pain tolerance, and fearlessness about death) and depression in males and females using meta-analysis and meta-analytic connectivity modeling. Existence of both ACS and depression (suicidal desire) being essential in an individual for lethal suicidal behavior according to IPTS, preliminary network containing regions corresponding to both ACS and Depression networks was identified. Diffusion tractography was implemented to identify the structural network underlying fatal suicidal behavior. Significant differences were found in ACS,

Depression and ACS-Depression functional as well as structural network between males and females.

Second goal of this thesis was to study canine model as they lie at an intermediate stage in the evolutionary hierarchy between primates and rodents and serve as a large animal model, critical for translation of MRI results to humans. Group-wise DTI based atlas was computed to account for inter-subject variability which can subsequently be utilized in future studies in translational research. Additionally, the hypothesis that functional finding regarding the anterior-posterior dissociation of the DMN in a previous study on canines might possess structural basis was tested. Low FA values found in the cingulate cortex (along the ACC-PCC axis) in dogs and extremely sparse fiber connections between ACC and PCC supported our hypothesis. Default mode network being implicated in self-referential processing and higher cognition in humans, might also suggest that evolution of higher cognitive functions in humans was supported by stronger functional and structural connectivity between anterior and posterior regions of the DMN.

Bibliography

[1] Blink E. "An easy introduction to Basic MRI Physics for anyone who does not have a degree in physics." *http://www.mri-physics.net/* (http://www.mri-physics.net/), 2004.

[2] Yoshioka H, Schlechtweg P and Kose K. "Magnetic Resonance Imaging." In *Imaging of Arthritis and Metabolic Bone Disease*, by Weissman BNW, 34-47. Philadelphia, PA: Mosby/Elsevier, 2009.

[3] Buschong SC. *Magnetic Resonance Imaging.* Elsevier Health Sciences, 2003.

[4] Liney, G.P. *What is MRI?* September 25, 2014. http://www2.hull.ac.uk/science/mri/whatismri.aspx (accessed March 18, 2015).

[5] Huettel S. A., Song A. W. and McCarthy G. *Functional magnetic resonance imaging.* Sunderland, MA: Sinauer Associates, 2004.

[6] Thulborn K R, Waterton J C, Matthews P M and Radda G K. "Oxygenation dependence of the transverse relaxation time of water protons in whole blood at high field." *Biochim. Biophys. Acta 714* , 1982: 265–70.

[7] Ogawa, S., Lee, T. M., Kay, A. R., & Tank, D. W. "Brain magnetic resonance imaging with contrast dependent on blood oxygenation." *Proceedings of the National Academy of Sciences of the United States of America, 87(24)*, 1990: 9868–9872.

[8] Einstein A. *Investigations on the theory of the brownian movement.* New York, NY: Dover, 1956.

[9] Johansen-Berg H, Behrens TEJ. *Diffusion MRI: From Quantitative Measurement to In vivo Neuroanatomy, Second Ed.* Oxford, UK: Academic Press, 2014.

[10] Koh DM, Collins DJ. "Diffusion-weighted MRI in the body: applications and challenges in oncology." *AJR Am J Roentgenol, 188(6)*, 2007: 1622-35.

[11] Rosenbloom M1, Sullivan EV, Pfefferbaum A. "Using magnetic resonance imaging and diffusion tensor imaging to assess brain damage in alcoholics." *Alcohol Res Health, 27(2)*, 2003: 146-52.

[12] D, Le Bihan. "Looking into the functional architecture of the brain with diffusion MRI." *Nat Rev Neurosci, 4(6)*, 2003: 469-80.

[13] Shrager RI, Basser PJ. "Anisotropically weighted MRI." *Magn Reson Med, 40(1)*, 1998: 160-5.

[14] Basser PJ, Mattiello J, LeBihan D. "Estimation of the effective self-diffusion tensor from the NMR spin echo." *J Magn Reson B, 103(3)*, 1994: 247-54.

[15] Basser PJ, Mattiello J, LeBihan D. "MR diffusion tensor spectroscopy and imaging." *Biophys J, 66(1)*, 1994: 259-67.

[16] Hagmann, P., Jonasson, L., Maeder, P., Thiran, J.P., Wedeen, V.J., Meuli, R. "Understanding Diffusion MR Imaging Techniques: From Scalar Diffusion-weighted Imaging to Diffusion Tensor Imaging and Beyond." *Radiographics, 26*, 2006: S205–S223.

[17] Pannek K, Guzzetta A, Colditz PB, Rose SE. "Diffusion MRI of the neonate brain: acquisition, processing and analysis techniques." *Pediatr Radiol, 42(10)*, 2012 : 1169-82.

[18] Alexander, A. L., Lee, J. E., Lazar, M., & Field, A. S. "Diffusion Tensor Imaging of the Brain." *Neurotherapeutics: The Journal of the American Society for Experimental NeuroTherapeutics, 4(3)* , 2007: 316–329.

[19] Conturo TE, Lori NF, Cull TS, Akbudak E, Snyder AZ, Shimony JS, McKinstry RC, Burton H, Raichle ME. "Tracking neuronal fiber pathways in the living human brain." *Proc Natl Acad Sci U S A, 96(18)*, 1999 : 10422-7.

[20] Basser PJ, Pajevic S, Pierpaoli C, Duda J, Aldroubi A. "In vivo fiber tractography using DT-MRI data." *Magn Reson Med, 44(4)*, 2000 : 625-32.

[21] Ahn S, Lee SK. "Diffusion tensor imaging: exploring the motor networks and clinical applications." *Korean J Radiol, 12(6)*, 2011: 651-61.

[22] Behrens TEJ, Woolrich MW, Jenkinson M, Johansen-Berg H, Nunes RG, Clare S, et al. "Characterization and propagation of uncertainty in diffusion-weighted MR imaging." *Magn Reson Med, 50(5)*, 2003: 1077-1088.

[23] Fling BW, Dutta GG, Schlueter H, Cameron MH, Horak FB. "Associations between Proprioceptive Neural Pathway Structural Connectivity and Balance in People with Multiple Sclerosis." *Front Hum Neurosci, 8.*, 2014: 814.

[24] Eickhoff SB, Laird AR, Grefkes C, Wang LE, Zilles K, Fox PT. "Coordinate-based activation likelihood estimation meta-analysis of neuroimaging data: A random-effects approach based on empirical estimates of spatial uncertainty." *Hum Brain Mapp 30*,

2009: 2907-2926.

[25] Eickhoff SB, Bzdok D, Laird AR, Kurth F, Fox PT. "Activation likelihood estimation revisited." *Neuroimage 59*, 2012: 2349-2361.

[26] Turkeltaub PE, Eickhoff SB, Laird AR, Fox M, Wiener M, Fox P. "Minimizing within-experiment and within-group effects in activation likelihood estimation meta-analyses." *Hum Brain Mapp 33*, 2012: 1-13.

[27] Drapeau, C. W., & McINtosh, J. L. *U.S. A. suicide 2012: Official final data.* American Association of Suicidology. 2014. www.suicidology.org (accessed 10 18, 2014).

[28] World Health Organization. *Suicide rates per 100,000 by Country, Year, and Sex.* 2011. www.who.int/mental_health/prevention/suicide_rates/en/index.html (accessed July 2, 2012).

[29] Piccinelli, M., & Wilkinson, G. " Gender differences in depression: Critical review." *British Journal of Psychiatry, 177*, 2000: 486-492.

[30] Van de Velde, S., Bracke, P., & Levecque, K. "Gender differences in depression in 23 European countries: Cross-national variation in the gender gap in depression." *Social Science & Medicine, 71*, 2010: 305-313.

[31] Nock, M. K., Bortes, G., Bromet, E. J., Alonso, J., Angermeyer, M., Beautrais, A…Williams, D. "Cross-national prevalence and risk factors for suicidal ideation, plans, and attempts." *The British Journal of Psychiatry, 192*, 2008: 98-105.

[32] Hawton, K. "Sex and suicide: Gender differences in suicidal behaviour." *The British Journal of Psychiatry, 177*, 2000: 484-485.

[33] Schrijvers, D. L., Bollen, J., & Sabbe, B. G. C. "The gender paradox in suicidal behavior and its impact on the suicidal process." *Journal of Affective Disorders, 138*, 2012: 19-26.

[34] Cibis, A., Mergl, R., Bramesfeld, A., ALthaus, D., Niklewski, G., Schmidtke, A., & Hegerl, U. "Preference of lethal methods is not the only cause for higher suicide rates in males." *Journal of Affective Disorders, 136*, 2012: 9-16.

[35] Ehrlich, S., Breeze, J., Hesdorffer, D., Noam, G., Hong, X., Alban, R…Renshaw, P. "White matter hyperintensities and their association with suicidality in depressed young adults." *Journal of Affective Disorders, 86*, 2005: 281-287.

[36] Pompili, M., Innamorati, M., Mann, J., Oquendo, M., Lester, D., Del Casale, A…Girardi,

P. "Periventricular white matter hyperintensities as predictors of suicide attempts in bipolar disorders and unipolar depression." *Progress in Neuro-Psychopharmacology and Biological Psychiatry, 32*, 2008: 1501-1507.

[37] Wagner, G., Koch, K., Schachtzabel, C., Schultz, C. C., Sauer, H., &Schlosser, R. G. "Structural brain alterations in patients with major depressive disorder and high risk for suicide: Evidence for a distinct neurobiological entity?" *Neuroimage, 54*, 2011: 1607-1614.

[38] Jollant, F., Lawrence, N., Olie, E., O'Daly, O., Malafosse, A., Courtet, P., & Phillips, M. "Decreased activation of lateral orbitofrontal cortex during risky choices under uncertainty is associated with disadvantageous decision-making and suicidal behavior." *Neuroimage, 51*, 2010: 1275-1281.

[39] Reisch, T., Seifritz, E., Esposito, F., Wiest, R., Valach, L., & Michel, K. "An fMRI study on mental pain and suicidal behavior." *Journal of Affective Disorders, 126*, 2010: 321-325.

[40] Oquendo, M., Hastings, R., Huang, Y., Simpson, N., Ogden, R., Hu, X., Goldman, D…Parsey, R. V. "Brain serotonin transporter binding in depressed patients with bipolar disorder using positron emission tomography." *Archives of General Psychiatry, 64*, 2007: 201-208.

[41] Oquendo, M., Placidi, G., Malone, K., Campbell, C., Keilp, J., Brodsky, B…Mann, J. J. "Positron emission tomography of regional brain metabolic responses to a serotonergic challenge and lethality of suicide attempts in major depression." *Archives of General Psychiatry, 60*, 2003: 14-22.

[42] Desmyter, S., van Heeringen, C., & Audenaert, K. "Structural and functional neuroimaging studies of the suicidal brain." *Progress in Neuro-psychopharmacology and Biological Psychiatry, 35*, 2011: 796-808.

[43] Van Heeringen, C., Bijttebier, S., & Godfrin, K. "Suicidal brains: A review of functional and structural brain studies in association with suicidal behavior." *Neuroscience and Biobehavioral Reviews, 35*, 2011: 688-698.

[44] Koenigs, M., & Grafman, J. "The functional neuroanatomy of depression: Distinct roles for ventromedial and dorsolateral prefrontal cortex." *Behavioural Brain Research, 201*, 2009: 239-243.

[45] McNally, R. J. "Cognitive abnormalities in post-traumatic stress disorder." *TRENDS in*

Cognitive Sciences,10, 2006: 271-277.

[46] Minzenberg, M. J., Laird, A. R., Thelen, S., Carter, C. S., & Glahn, D. C. "Meta-analysis of 41 functional neuroimaging studies of executive function in schizophrenia." *Archives of General Psychiatry, 66*, 2009: 811-822.

[47] Arango, V., Underwood, M. D., Gubbi, A. V., & Mann, J. J. "Localized alterations in pre- and postsynaptic serotonin binding sties in the ventrolateral prefrontal cortex of suicide victims." *Brain Research 688*, 1995: 121-133.

[48] Mann, J., Huang, Y., Underwood, M., Kassir, S., Oppenheim, S., Kelly, T…Arango, V. "A serotonin transporter gene promoter polymorphism (5-HTTLPR) and prefrontal cortical binding in major depression and suicide." *Archives of General Psychiatry, 57*, 2000: 729-738.

[49] Amen, D. G., Prunella, J. R., Fallon, J. H., Amen, B., & Hanks, C. "A comparative analysis of completed suicide using high resolution brain SPECT imaging. ." *The Journal of Neuropsychiatry and Clinical Neurosciences, 21*, 2009: 430-439.

[50] Courtet, P., Gottesman, I. I., Jollant, F., & Gould, T. D. "The neuroscience of suicidal behaviors: What can we expect from endophenotype strategies?" *Translational Psychiatry, 1* e7 (2011).

[51] Joiner, T. E. *Why People Die By Suicide.* Cambridge, MA: Harvard University Press, 2005.

[52] Van Orden, K. A., Witte, T. K., Cukrowicz, K. C., Braithwaite, S. R., Selby, E. A., & Joiner, T. E. "The interpersonal theory of suicide." *Psychological Review, 117*, 2010: 575-600.

[53] Smith, P. N., Cukrowicz, K. C., Poindexter, E. K., Hobson, V., & Cohen, L. M. "The acquired capability for suicide: A comparison of suicide attempters, suicide ideators, and non-suicidal controls." *Depression & Anxiety, 27*, 2010: 871-877.

[54] Cambron, M. J., Acitelli, L. K., & Pettit, J. W. " Explaining gender differences in depression: An interpersonal contingent self-esteem perspective." *Sex Roles,61*, 2009: 751-761.

[55] Cyranowski, J. M., Frank, E., Young, E., & Shear, K. "Adolescent onset of the gender difference in lifetime rates of major depression: A theoretical model." *Archives of General Psychiatry, 57*, 2000: 21-27.

[56] Ribeiro, J. D., Witte, T. K., Van Orden, K. A., Selby, E. A., Gordon, K., Bender, T. W., & Joiner, T. E. "Fearlessness about death: The psychometric properties and construct validity of the revision to the Acquired Capability for Suicide Scale." *Psychological Assessment, 26*, 2014: 115-126.

[57] Witte, T. K., Gordon, K. H., Smith, P. N., & Van Orden, K. A. "Stoicism and sensation seeking: Male vulnerabilities for the acquired capability for suicide." *Journal of Research in Personality, 46*, 2012: 384-392.

[58] Bender, T. W., Gordon, K. H., Bresin, K., & Joiner, T. E. " Impulsivity and suicidality: The mediating role of painful and provocative experiences." *Journal of Affective Disorders, 129*, 2011: 301-307.

[59] Bryan, C. J., Cukrowicz, K. C., West, C. L., & Morrow, C. E. "Combat experience and the acquired capability for suicide." *Journal of Clinical Psychology, 66*, 2010: 1044-1056.

[60] Dumais, A., Lesage, A. D., Alda, M., Rouleau, G., Dumont, M., Chawky, N…Turecki, G. "Risk factors for suicide completion in major depression: A case control study of impulsive and aggressive behaviors in men." *The American Journal of Psychiatry, 162*, 2005: 2116-2124.

[61] Kang, H. K., & Bullman, T. A. "Risk of suicide among US veterans after returning from the Iraq or Afghanistan war zones." *Journal of the American Medical Association, 300*, 2008: 652-653.

[62] Cheng, C. "Marginalized masculinities and hegemonic masculinity: An introduction." *Journal of Men's Studies, 7*, 1999: 295.

[63] David, D., & Brannon, R. (Eds). *The forty-nine percent majority: The male sex role.* Reading, MA: Addison-Wesley, 1976.

[64] Murray, G., Judd, F., Jackson, H., Fraser, C., Komiti, A., Pattison, P., W…Robins, G. "Big boys don't' cry: An investigation of stoicism and its mental health outcomes." *Personality and Individual Differences, 4*, 2008: 1369-1381.

[65] Roberti, J. W. "A review of behavioral and biological correlates of sensation seeking." *Journal of Research in Personality, 38*, 2004: 256-279.

[66] Kunz, M., Chen, J. I., Lautenbacher, S., Vachon-Presseau, E., & Rainville, P. "Cerebral regulation of facial expressions of pain." *The Journal of Neuroscience, 31*, 2011: 8730-

8738.

[67] Robinson, M. E., Riley, J. L., Myers, C. D., Papas, R. K., Wise, E. A., Waxenberg, L. B., et al. "Gender role expectations of pain: Relationship to sex differences in pain." *The Jouranl of Pain, 2*, 2001: 251-257.

[68] Wise, E. A., Price, D. D., Myers, D. C., Heft, W. M., & Robinson, E. M. . "Gender role expectations of pain: Relationship to experimental pain perception." *Pain, 96*, 2002: 335-342.

[69] Yong, H. H. "Can attitudes of stoicism and cautiousness explain observed age-related variation in levels of self-rated pain, mood disturbance, and functional interference in chronic pain patients?" *European Journal of Pain, 10*, 2006: 399-407.

[70] Laird AR, Lancaster JL, Fox PT. "BrainMap: The social evolution of a functional neuroimaging database." *Neuroinformatics 3*, 2005: 65-78.

[71] Fox PT, Lancaster JL. "Mapping context and content: The BrainMap model." *Nature Rev Neurosci 3*, 2002: 319-321.

[72] Fox PT, Laird AR, Fox SP, Fox PM, Uecker AM, Crank M, Koenig SF, Lancaster JL. "BrainMap taxonomy of experimental design: Description and evaluation." *Hum Brain Mapp 25*, 2005: 185-198.

[73] Laird, A., Eickhoff, S., Fox, P. M., Uecker, A., Ray, K., Saenz, J., . . . Fox, P. "The BrainMap strategy for standardization, sharing, and meta-analysis of neuroimaging data." *BMC Research Notes, 4*, 2011: 349.

[74] Laird, A. R., Fox, P. M., Price, C. J., Glahn, D. C., Uecker, A. M., Lancaster, J. L., . . . Fox, P. T. "ALE meta-analysis: Controlling the false discovery rate and performing statistical contrasts." *Human Brain Mapping, 25(1)*, 2005: 155-164.

[75] Robinson, J. L., Laird, A. R., Glahn, D. C., Lovallo, W. R., & Fox, P. T. "Meta-analytic connectivity modeling: Delineating the functional connectivity of the human amygdala." *Human Brain Mapping, 31(2)*, 2010: 173-184.

[76] Robinson JL, Laird AR, Glahn DC, Blangero J, Sanghera MK, Pessoa L, Fox PM, Uecker A, Friehs G, Young KA, Griffin JL, Lovallo WR, Fox PT. "The functional connectivity of the human caudate: an application of meta-analytic connectivity modeling with behavioral filtering." *NeuroImage, 60(1)*, 2012: 117-129.

[77] Smith S.M., Zhang Y., Jenkinson M., Chen J., Matthews P.M., Federico A., and De

Stefano N. "Accurate, robust and automated longitudinal and cross-sectional brain change analysis." *NeuroImage, 17(1)*, 2002: 479-489.

[78] Behrens TEJ, Johansen-Berg H, Woolrich MW, Smith SM, Wheeler-Kingshott CAM, Boulby PA, et al. "Non-invasive mapping of connections between human thalamus and cortex using diffusion imaging." *Nature Neuroscience, 6(7)*, 2003: 750-757.

[79] Johansen-Berg H, Behrens TEJ, Robson MD, Drobnjak I, Rushworth MFS, Brady JM, et al. "Changes in connectivity profiles define functionally distinct regions in human medial frontal cortex." *Proc Natl Acad Sci U S A, 101(36)*, 2004: 13335-13340.

[80] Zeki S, Romaya JP. "Neural Correlates of Hate." *PLoS ONE 3(10): e3556*, 2008.

[81] Stevens, J. S., & Hamann, S. . "Sex differences in brain activation to emotional stimuli: a meta-analysis of neuroimaging studies." *Neuropsychologia, 50*, 2012: 1578–1593.

[82] Hadland, K. A., Rushworth M.F., et al. "The effect of cingulate lesions on social behaviour and emotion." *Neuropsychologia 41(8)*, 2003: 919–931.

[83] Fitzgerald, P. B., Laird, A. R., Maller, J., & Daskalakis, Z. J. "A Meta-Analytic Study of Changes in Brain Activation in Depression." *Human Brain Mapping, 29(6) doi:10.1002/hbm.20426*, 2008: 683–695.

[84] Graham J., Salimi-Khorshidi G., Hagan C., Walsh N., Goodyer I., Lennox B., et al. "Meta-analytic evidence for neuroimaging models of depression: state or trait?" *J. Affect. Disord. 151 .10.1016/j.jad.2013.07.002*, 2013: 423–431.

[85] Palmer, S. M., Crewther, S. G., Carey, L. M., & The START Project Team. "A Meta-Analysis of Changes in Brain Activity in Clinical Depression." *Frontiers in Human Neuroscience, 8 doi:10.3389/fnhum.2014.01045*, 2014: 1045.

[86] Berlim, M. T., Van den Eynde, F., & Jeff Daskalakis, Z. "Clinically Meaningful Efficacy and Acceptability of Low-Frequency Repetitive Transcranial Magnetic Stimulation (rTMS) for Treating Primary Major Depression: A Meta-Analysis of Randomized, Double-Blind and Sham-Controlled Trials." *Neuropsychopharmacology 38(4)*, 2013: 543–551.

[87] Van Heeringen, K., Bijttebier, S., Desmyter, S., Vervaet, M., & Baeken, C. "Is there a neuroanatomical basis of the vulnerability to suicidal behavior? A coordinate-based meta-analysis of structural and functional MRI studies." *Frontiers in Human Neuroscience, 8*, 2014: 824.

[88] Talati A, Hirsch J. "Functional specialization within the medial frontal gyrus for perceptual go/no-go decisions based on "what," "when," and "where" related information: an fMRI study." *J Cogn Neurosci 17 (7)*, 2005: 981–93.

[89] Northoff G, Walter M, Schulte RF, Beck J, Dydak U, et al. "GABA concentrations in the human anterior cingulate cortex predict negative BOLD responses in fMRI." *Nat Neurosci 10 17982452*, 2007: 1515–1517.

[90] Harris, A. D., Puts, N. A. J., Anderson, B. A., Yantis, S., Pekar, J. J., Barker, P. B., & Edden, R. A. E. "Multi-Regional Investigation of the Relationship between Functional MRI Blood Oxygenation Level Dependent (BOLD) Activation and GABA Concentration." *PLoS ONE, 10(2) e0117531*, 2015.

[91] Laird, A. R., Eickhoff, S. B., Kurth, F., Fox, P. M., Uecker, A. M., Turner, J. A., . . . Fox, P. T. "ALE meta-analysis workflows via the BrainMap database: Progress towards a probabilistic functional brain atlas." *Frontiers in Neuroinformatics, 3*, 2009: 1-11.

[92] Le Bihan D, Breton' E. "Imagerie de diffusion in-vivo par résonance." *C R Acad Sci (Paris) 301 (15)*, 1985: 1109–1112.

[93] Merboldt KD, Hanicke W, Frahm J. "Diffusion imaging using stimulated echoes." *Magn. Reson. Med., 19*, 1991: 233–239.

[94] Taylor DG, Bushell MC. "The spatial mapping of translational diffusion coefficients by the NMR imaging technique." *Phys. Med. Biol. 30(4)*, 1985: 345-9.

[95] Baloch S, Verma R, Huang H, Khurd P, Clark S, Yarowsky P, et al. "Quantification of Brain Maturation and Growth Patterns in C57BL/6J Mice via Computational Neuroanatomy of Diffusion Tensor Images." *Cerebral Cortex (New York, NY), 19(3)*, 2009: 675–687.

[96] Jacqmot O, Van Thielen B, Fierens Y, Hammond M, Willekens I, Schuerbeek PV, et al. "Diffusion Tensor Imaging of White Matter Tracts in the Dog Brain." *Anat Rec, 296*, 2013: 340–349.

[97] Anaya García M S, Hernández Anaya J S, Marrufo Meléndez O, Velázquez Ramírez J L and Palacios Aguiar R. "In vivo study OF cerebral white matter in the dog using diffusion tensor tractography." *Veterinary Radiology & Ultrasound*, 2014.

[98] Wu YC, Field AS, Duncan ID, Samsonov AA, Kondo Y, Tudorascu D, et al. "High b-value and diffusion tensor imaging in a canine model of dysmyelination and brain

maturation." *Neuroimage. 58(3)*, 2011: 829-37.

[99] Kingfisher. Biotech Inc. *Kingfisher Biotech Circular Subject: Canine as an Animal Model Volume 1; No. 1* . http://www.kingfisherbiotech.com/newsletter/Canine_Animal_Model_Newsletter.pdfhttp ://www.kingfisherbiotech.com/newsletter/Canine_Animal_Model_Newsletter.pdf (accessed March 18, 2015).

[100] Centers for Disease Control and Prevention. . *Rabies. Other Wild Animals: Terrestrial carnivores: raccoons, skunks and foxes.* November 15, 2011. http://www.cdc.gov/rabies/exposure/animals/other.html (accessed March 18, 2015).

[101] Reid, PJ. "Adapting to the human world: dogs' responsiveness to our social cues." *Behav Processes, 80(3)*, 2009: 325-33.

[102] Soproni, Krisztina, Ádám Miklósi, József Topál, and Vilmos Csányi. "Dogs' (Canis familaris) responsiveness to human pointing gestures." *Journal of Comparative Psychology, Vol 116(1)*, 2002: 27-34.

[103] Hare B, Tomasello M. "Human-like social skills in dogs?" *Trends Cogn Sci, 9(9)*, 2005: 439-44.

[104] Lazarowski L, Dorman DC. "A comparison of pet and purpose-bred research dog (Canis familiaris) performance on human-guided object-choice tasks." *Behav Processes, 110*, 2015 : 60-7.

[105] Hasegawa D, Yamato O, Nakamoto Y, Ozawa T, Yabuki A, Itamoto K, et al. "Serial MRI Features of Canine GM1 Gangliosidosis: A Possible Imaging Biomarker for Diagnosis and Progression of the Disease." *The Scientific World Journal, 250197*, 2012.

[106] Laothamatas J, Sungkarat W, Hemachudha T. "Neuroimaging in rabies." *Advances in Virus Research Volume 79*, 2011: 309–327.

[107] Kyathanahally S, Jia H, Pustovyy OM, Waggoner P, Beyers R, Schumacher J, et al. "Anterior–posterior dissociation of the default mode network in dogs." *Brain Structure and Function. Volume 220, Issue 2* , 2015: pp 1063-1076.

[108] Mantini D, Gerits A, Nelissen K, Durand JB, Joly O, Simone L, et al. "Default mode of brain function in monkeys." *J Neurosci, 31(36)*, 2011: 12954–62.

[109] Greicius MD, Krasnow B, Reiss AL, Menon V. "Functional connectivity in the resting brain: A network analysis of the default mode hypothesis." *Proceedings of the National*

Academy of Sciences of the United States of America, 100(1), 2003: 253–258.

[110] Fox MD, Raichle ME. "Spontaneous fluctuations in brain activity observed with functional magnetic resonance imaging." *Nat Rev Neurosci 8* , 2007: 700–711.

[111] Raichle ME, MacLeod AM, Snyder AZ, Powers WJ, Gusnard DA, Shulman GL. "A default mode of brain function." *Proc Natl Acad Sci USA 98*, 2001: 676–682.

[112] Buckner RL, Andrews-Hanna JR, Schacter DL. "The brain's default network: anatomy, function, and relevance to disease." *Ann N Y Acad Sci 1124*, 2008: 1–38.

[113] Fransson P, Marrelec G. "The precuneus/posterior cingulate cortex plays a pivotal role in the default mode network: Evidence from a partial correlation network analysis." *Neuroimage 42*, 2008: 1178–1184.

[114] Mitchell JP, Heatherton TF, Macrae CN. "Distinct neural systems subserve person and object knowledge." *Proc Natl Acad Sci U S A., 99(23)*, 2002: 15238-43.

[115] Lou HC, Luber B, Crupain M, Keenan JP, Nowak M, Kjaer TW,et al. "Parietal cortex and representation of the mental Self." *Proc Natl Acad Sci U S A., 101(17)*, 2004: 6827-32.

[116] Lundstrom BN, Ingvar M, Petersson KM. "The role of precuneus and left inferior frontal cortex during source memory episodic retrieval." *Neuroimage., 27(4)*, 2005: 824-34.

[117] Greicius, M. "Resting-state functional connectivity in neuropsychiatric disorders." *Curr Opin Neurol 21*, 2008: 424–430.

[118] Gusnard DA, Raichle ME. "Searching for a baseline: functional imaging and the resting human brain." *Nat Rev Neurosci 2*, 2001: 685–694.

[119] Becerra L, Pendse G, Chang P-C, Bishop J, Borsook D. "Robust reproducible resting state networks in the awake rodent brain." *PloS One 6(10):e25701*, 2011.

[120] Lu H, Zou Q, Gu H, Raichle ME, Steina EA, Yanga Y. "Rat brains also have a default mode network." *Proc Natl Acad Sci USA 109(10)*, 2011: 3979–3984.

[121] Upadhyay J, Baker SJ, Chandran P, Miller L, Lee Y, Marek GJ, et al. "Default-mode-like network activation in awake rodents." *PloS One 6(11):e27839*, 2011.

[122] Horn A, Ostwald D, Reisert M, Blankenburg F. "The structural-functional connectome and the default mode network of the human brain." *NeuroImage 13* , 2013: 1053–8119.

[123] Smith SM, Jenkinson M , Woolrich MW , Beckmann CF, Behrens TEJ, Johansen-Berg H, et al. "Advances in functional and structural MR image analysis and implementation as FSL." *NeuroImage, 23(S1)*, 2004: 208-19.

[124] Woolrich MW, Jbabdi S, Patenaude B, Chappell M, Makni S, Behrens T, et al. "Bayesian analysis of neuroimaging data in FSL." *NeuroImage, 45*, 2009: S173-86.

[125] Jenkinson M, Beckmann CF, Behrens TE, Woolrich MW, Smith SM. "FSL." *NeuroImage, 62*, 2012: 782-90.

[126] Jenkinson M, Pechaud M, Smith S. "ET2: MR-based estimation of brain, skull and scalp surfaces." , 2005.

[127] Datta R, Lee J, Duda J, Avants BB, Vite CH, Tseng B, et al. "A digital atlas of the dog brain." *PLoS ONE 7(12):e52140*, 2012.

[128] Jenkinson, M., Bannister, P., Brady, J. M. and Smith, S. M. "Improved Optimisation for the Robust and Accurate Linear Registration and Motion Correction of Brain Images." *NeuroImage, 17(2)*, 2002: 825-841.

[129] Jenkinson M, Smith S. "A Global Optimisation Method for Robust Affine Registration of Brain Images." *Medical Image Analysis, 5(2)*, 2001: 143-156.

[130] Greve DN, Fischl B. "Accurate and robust brain image alignment using boundary-based registration." *NeuroImage, 48(1)*, 2009: 63-72.

[131] Alexander DC, Basser PJ, Pierpaoli C, Gee JC. "Spatial transformations of diffusion tensor Images." *IEEE Trans. Med. Imag.20(11)*, 2001: 1131–1139.

[132] Supekar K, Uddin LQ, Prater K, Amin H, Greicius MD, Menon V. "Development of functional and structural connectivity within the default mode network in young children." *Neuroimage 52(1)*, 2010: 290–301.

[133] Merola I, Prato-Previde E, Marshall-Pescini S. "Dogs' social referencing towards owners and strangers." *PLoS One, 7(10):e47653*, 2012.

[134] Li W, Mai X, Liu C. "The default mode network and social understanding of others: what do brain connectivity studies tell us." *Front Hum Neurosci, 8:74*, 2014.

[135] Che X, Zhang Q, Zhao J, Wei D, Li B, Guo Y, Qiu J, Liu Y. "Synchronous activation within the default mode network correlates with perceived social support." *Neuropsychologia, 63*, 2014: 26-33.

[136] Greicius MD, Supekar K, Menon V, Dougherty RF. "Resting-State Functional Connectivity Reflects Structural Connectivity in the Default Mode Network." *Cerebral Cortex (New York, NY), 19(1)*, 2009: 72–78.

[137] Laothamatas J, Sungkarat W, Hemachudha T. "Research Advances in Rabies." *Advances in Virus Research Volume 79*, 2011: 309–327.

[138] Zuckerman, M., Eysenck, S., & Eysenck, H. J. "Sensation seeking in England and America: Cross-cultural, age, and sex comparisons." *Journal of Consulting and Clinical Psychology, 46*, 1978: 139-149.

[139] Smith, A. R., Ribeiro, J. D., Mikolajewski, A., Taylor, J., Joiner, T. E., & Iacono, W. G. "An examination of environmental and genetic contributions to the determinants of suicidal behavior among male twins." *Psychiatry Research, 197*, 2012: 60-65.

[140] Merboldt KD, Hanicke W, Frahm J. "Diffusion imaging using stimulated echoes." *Magn. Reson. Med. 19*, 1991: 233–239.

[141] Bushell, D G Taylor and M C. "The spatial mapping of translational diffusion coefficients by the NMR imaging technique." *Phys. Med. Biol. 30* , 1985: 345.

[142] Baloch, S., Verma, R., Huang, H., Khurd, P., Clark, S., Yarowsky, P., Davatzikos, C. "Quantification of Brain Maturation and Growth Patterns in C57BL/6J Mice via Computational Neuroanatomy of Diffusion Tensor Images." *Cerebral Cortex (New York, NY), 19(3)* , 2009: 675–687.

[143] Wu YC, Field AS, Duncan ID, Samsonov AA, Kondo Y, Tudorascu D, Alexander AL. "High b-value and diffusion tensor imaging in a canine model of dysmyelination and brain maturation." *Neuroimage. 58(3)*, 2011: 829-37.

[144] Hasegawa, D., Yamato, O., Nakamoto, Y., Ozawa, T., Yabuki, A., Itamoto, K., Orima, H. "Serial MRI Features of Canine GM1 Gangliosidosis: A Possible Imaging Biomarker for Diagnosis and Progression of the Disease." *The Scientific World Journal, 2012, 250197*, 2012.

[145] Laothamatas J, Sungkarat W, Hemachudha T. "Research Advances in Rabies." *Advances in Virus Research Volume 79* , 2011: 309–327.

[146] Jacqmot, O., Van Thielen, B., Fierens, Y., Hammond, M., Willekens, I., Schuerbeek, P. V., Verhelle, F., Goossens, P., De Ridder, F., Clarys, J. P., Vanbinst, A. and De Mey, J. "Diffusion Tensor Imaging of White Matter Tracts in the Dog Brain. ." *Anat Rec, 296* ,

2013: 340–349.

[147] Anaya García, M. S., Hernández Anaya, J. S., Marrufo Meléndez, O., Velázquez Ramírez, J. L. and Palacios Aguiar, R. "IN VIVO STUDY OF CEREBRAL WHITE MATTER IN THE DOG USING DIFFUSION TENSOR TRACTOGRAPHY." *Veterinary Radiology & Ultrasound.*, 2014.

[148] Kyathanahally S, Jia H, Pustovyy OM, Waggoner P, Beyers R, Schumacher J, Barrett J, Morrison EE, Salibi N, Denney TS, Vodyanoy VJ, Deshpande G. "Anterior–posterior dissociation of the default mode network in dogs." *Brain Structure and Function. Volume 220, Issue 2, pp 1063-1076*, 2015.

[149] Mantini D et al. "Default mode of brain function in monkeys." *J Neurosci 31(36):12954–12962*, 2011.

[150] Fox MD, Raichle ME. "Spontaneous fluctuations in brain activity observed with functional magnetic resonance imaging." *Nat Rev Neurosci 8: 700–711*, 2007.

[151] Raichle ME, MacLeod AM, Snyder AZ, Powers WJ, Gusnard DA, Shulman GL. "A default mode of brain function." *Proc Natl Acad Sci USA 98:676–682*, 2001.

[152] Buckner RL, Andrews-Hanna JR, Schacter DL. "The brain's default network: anatomy, function, and relevance to disease." *Ann N Y Acad Sci 1124:1–38*, 2008.

[153] Greicius, M. "Resting-state functional connectivity in neuropsychiatric disorders." *Curr Opin Neurol 21:424–430*, 2008.

[154] Gusnard DA, Raichle ME. "Searching for a baseline: functional imaging and the resting human brain." *Nat Rev Neurosci 2:685–694*, 2001.

[155] Becerra L, Pendse G, Chang P-C, Bishop J, Borsook D. "Robust reproducible resting state networks in the awake rodent brain." *PloS One 6(10):e25701.*, 2011.

[156] Lu H, Zou Q, Gu H, Raichle ME, Steina EA, Yanga Y. "Rat brains also have a default mode network." *Proc Natl Acad Sci USA 109(10):3979–3984*, 2011.

[157] Upadhyay J et al. "Default-mode-like network activation in awake rodents." *PloS One 6(11):e27839*, 2011.

[158] Smith S.M., Jenkinson M. , Woolrich M.W. , Beckmann C.F., Behrens T.E.J., Johansen-Berg H., Bannister P.R., De Luca M., Drobnjak I., Flitney D.E. , Niazy R., Saunders J., Vickers J., Zhang Y., De Stefano N., Brady J.M., and Matthews P.M. . "Advances in

functional and structural MR image analysis and implementation as FSL." *NeuroImage, 23(S1):208-19* , 2004.

[159] Woolrich M.W., Jbabdi S., Patenaude B., Chappell M., Makni S., Behrens T., Beckmann C., Jenkinson M., Smith S.M. " Bayesian analysis of neuroimaging data in FSL." *NeuroImage, 45:S173-86,* , 2009.

[160] Jenkinson M., Beckmann C.F., Behrens T.E., Woolrich M.W., Smith S.M. " FSL." *NeuroImage, 62:782-90,* , 2012.

[161] Datta R et al. "A digital atlas of the dog brain." *PLoS ONE 7(12):e52140*, 2012.

[162] Supekar K, Uddin LQ, Prater K, Amin H, Greicius MD, Menon V. "Development of functional and structural connectivity within the default mode network in young children." *Neuroimage 52(1):290–301*, 2010.

[163] Greicius M. D., Supekar K., Menon V., & Dougherty R. F. "Resting-State Functional Connectivity Reflects Structural Connectivity in the Default Mode Network." *Cerebral Cortex (New York, NY), 19(1), 72–78.*, (2009.

[164] Greicius M. D., Krasnow B., Reiss A. L., Menon V. "Functional connectivity in the resting brain: A network analysis of the default mode hypothesis." *24. Proceedings of the National Academy of Sciences of the United States of America, 100(1)*, 2003: 253–258.

[165] Behrens T.E.J., Woolrich M.W., Jenkinson M., Johansen-Berg H., Nunes R.G., Clare S., Matthews P.M., Brady J.M., and Smith S.M. "Characterization and propagation of uncertainty in diffusion-weighted MR imaging." *Magn Reson Med, 50(5):1077-1088*, 2003.

[166] Behrens T.E.J., Johansen-Berg H., Woolrich M.W., Smith S.M., Wheeler-Kingshott C.A.M., Boulby P.A., Barker G.J., Sillery E.L., Sheehan K., Ciccarelli O., Thompson A.J., Brady J.M., and Matthews P.M.,. "Non-invasive mapping of connections between human thalamus and cortex using diffusion imaging." *Nature Neuroscience, 6(7):750-757* , 2003.

[167] Johansen-Berg H., Behrens T.E.J., Robson M.D., Drobnjak I., Rushworth M.F.S., Brady J.M., Smith S.M., Higham D.J., and Matthews P.M. "Changes in connectivity profiles define functionally distinct regions in human medial frontal cortex." *Proc Natl Acad Sci U S A, 101(36):13335-13340*, 2004.

[168] Jenkinson, M., Bannister, P., Brady, J. M. and Smith, S. M. "Improved Optimisation for the Robust and Accurate Linear Registration and Motion Correction of Brain Images."

NeuroImage, 17(2), 825-841, ., 2002.

[169] Jenkinson, M. and Smith, S. M. " A Global Optimisation Method for Robust Affine Registration of Brain Images." *Medical Image Analysis, 5(2), 143-156* ., 2001.

[170] Greve, D.N. and Fischl, B. "Accurate and robust brain image alignment using boundary-based registration." *NeuroImage, 48(1):63-72.*, 2009.

[171] Horn A, Ostwald D, Reisert M, Blankenburg F. "The structural-functional connectome and the default mode network of the human brain." *NeuroImage 13: 1053–8119*, 2013.

[172] Alexander DC, Basser PJ, Pierpaoli C, Gee JC. "Spatial transformations of diffusion tensor Images." *IEEE Trans. Med. Imag.20(11): 1131–1139.*, 2001.

[173] Le Bihan, D, Breton', E. "Imagerie de diffusion in-vivo par résonance." *C R Acad Sci (Paris) 301 (15)*, 1985: 1109–1112.

[174] Fransson P, Marrelec G. "The precuneus/posterior cingulate cortex plays a pivotal role in the default mode network: Evidence from a partial correlation network analysis." *Neuroimage 42: 1178–1184.*, 2008.

[175] Mitchell JP, Heatherton TF, Macrae CN. "Distinct neural systems subserve person and object knowledge." *Proc Natl Acad Sci U S A.; 99(23):15238-43.*, 2002.

[176] Lou HC, Luber B, Crupain M, Keenan JP, Nowak M, Kjaer TW, Sackeim HA, Lisanby SH. "Parietal cortex and representation of the mental Self." *Proc Natl Acad Sci U S A.; 101(17):6827-32.*, 2004.

[177] Lundstrom BN, Ingvar M, Petersson KM. "The role of precuneus and left inferior frontal cortex during source memory episodic retrieval." *Neuroimage.; 27(4):824-34.*, 2005.